ERDC/GSL TR-13-35

Geotechnical and Structures Laboratory

US Army Corps of Engineers®
Engineer Research and Development Center

ERDC
INNOVATIVE SOLUTIONS for a safer, better world

# Comparing Production and Placement of Warm-Mix Asphalt to Traditional Hot-Mix Asphalt for Constructing Airfield Pavements

John F. Rushing, Mariely Mejías-Santiago, and Jesse D. Doyle

August 2013

ERDC/GSL TR-13-35
August 2013

# Comparing Production and Placement of Warm-Mix Asphalt to Traditional Hot-Mix Asphalt for Constructing Airfield Pavements

John F. Rushing, Mariely Mejías-Santiago, and Jesse D. Doyle

*Geotechnical and Structures Laboratory*
*US Army Engineer Research and Development Center*
*3909 Halls Ferry Road*
*Vicksburg, MS 39180-6199*

Final report



Prepared for US Air Force Civil Engineer Center
139 Barnes Drive, Suite 1
Tyndall AFB, FL 32403-5319

# Abstract

Warm-mix asphalt (WMA) is an emerging technology that allows for production and placement of asphalt concrete at lower temperatures than conventional hot-mix asphalt (HMA). Full-scale pavement test sections were constructed using conventional equipment to observe differences in the techniques used to produce, place, and compact asphalt concrete using warm mixtures. These observations are needed to ensure construction specifications are adjusted appropriately for WMA construction. Results from this phase of the study include data identifying differences in WMA and HMA construction. The WMA was successfully constructed using the same equipment to produce in-place density equivalent to the HMA at reduced temperatures. Future work will include trafficking the pavement sections using accelerated pavement testing equipment to determine the WMA rutting performance.

# Contents

# Figures and Tables

## Figures

## Tables

# Preface

The US Army Engineer Research and Development Center (ERDC) was tasked by US Air Force Civil Engineering Center (AFCEC) to evaluate warm mix asphalt (WMA) for airfield pavements. The study was divided into three phases: laboratory evaluation, plant production and construction, and performance testing. The results from the plant production and construction evaluation are presented in this report.

This publication was prepared by personnel of ERDC's, Geotechnical and Structures Laboratory (GSL), Engineering Systems and Materials Division (ESMD), Airfields and Pavements Branch (APB). The findings and recommendations presented in this report are based upon the results of tests conducted on full-scale test items constructed at ERDC during June 2012. The principal investigators for this study were Mariely Mejías-Santiago, Dr. Jesse D. Doyle, and John F. Rushing, APB. The research team included Quint S. Mason, APB; Tim McCaffrey, Lance Warnock, and Kevin Taylor, Concrete and Materials Branch (CMB); and Harold T. Carr and Tony N. Brogdon, ERDC Information Technology Laboratory (ITL). Rushing, Mejías-Santiago, and Doyle prepared this publication under the supervision of Dr. Gary L. Anderton, Chief, APB; Dr. Larry N. Lynch, Chief, ESMD; Dr. William P. Grogan, Deputy Director, GSL; and Dr. David W. Pittman, Director, GSL.

COL Kevin J. Wilson was Commander of ERDC. Dr. Jeffery P. Holland was Director.

# Unit Conversion Factors

| Multiply | By | To Obtain |
|---|---|---|
| degrees Fahrenheit | (F-32)/1.8 | degrees Celsius |
| feet | 0.3048 | meters |
| inches | 0.0254 | meters |
| kips (force) per square inch | 6.894757 | megapascals |
| pounds (force) per square inch | 6.894757 | kilopascals |
| pounds (mass) | 0.45359237 | kilograms |

# 1 Introduction

## Background

Over the last several years, the hot mix asphalt (HMA) industry has focused on developing and identifying emerging technologies that reduce the environmental impact during production of bituminous paving materials. One technology, warm mix asphalt (WMA), is gaining popularity and acceptance by the HMA industry and has replaced HMA for many paving projects in recent years. In general terms, WMA is an asphalt concrete produced at lower temperatures than conventional HMA. Many techniques have been developed to produce WMA, including chemical additives, organic wax additives, and foaming agents. State departments of transportation (DOTs) are quickly adopting WMA for roadway paving, and many are using it in place of conventional HMA. As state DOTs gain experience with WMA, conventional HMA may become less available for paving. Thus, the material must be evaluated to determine its suitability for airfield paving operations.

## Previous work

The study presented in this report is part of a larger research effort that has been conducted to evaluate WMA technologies and provide guidance on their use for airfield pavements. A general description of the WMA research is summarized in the following paragraphs and presented in the flow chart in Figure 1.

In FY10, a team of researchers at the US Army Engineer Research and Development Center (ERDC) was tasked with evaluating the laboratory performance of different WMA technologies in order to certify their use for airfield pavements. The performance of mixtures produced in the lab using different WMA technologies was compared to the performance of the same mixtures produced at standard HMA production temperatures. Properties assessed included susceptibility to permanent deformation, moisture damage and low-temperature cracking, durability, and workability. The use of high-recycled asphalt pavement (RAP) contents was also evaluated. Results of the testing and evaluation indicated that WMA is a viable product for airfield pavement surface mixtures, and based on those findings a Unified Facilities Guide Specification (UFGS 32 12 15.16) and an

Figure 1. WMA research flow chart.

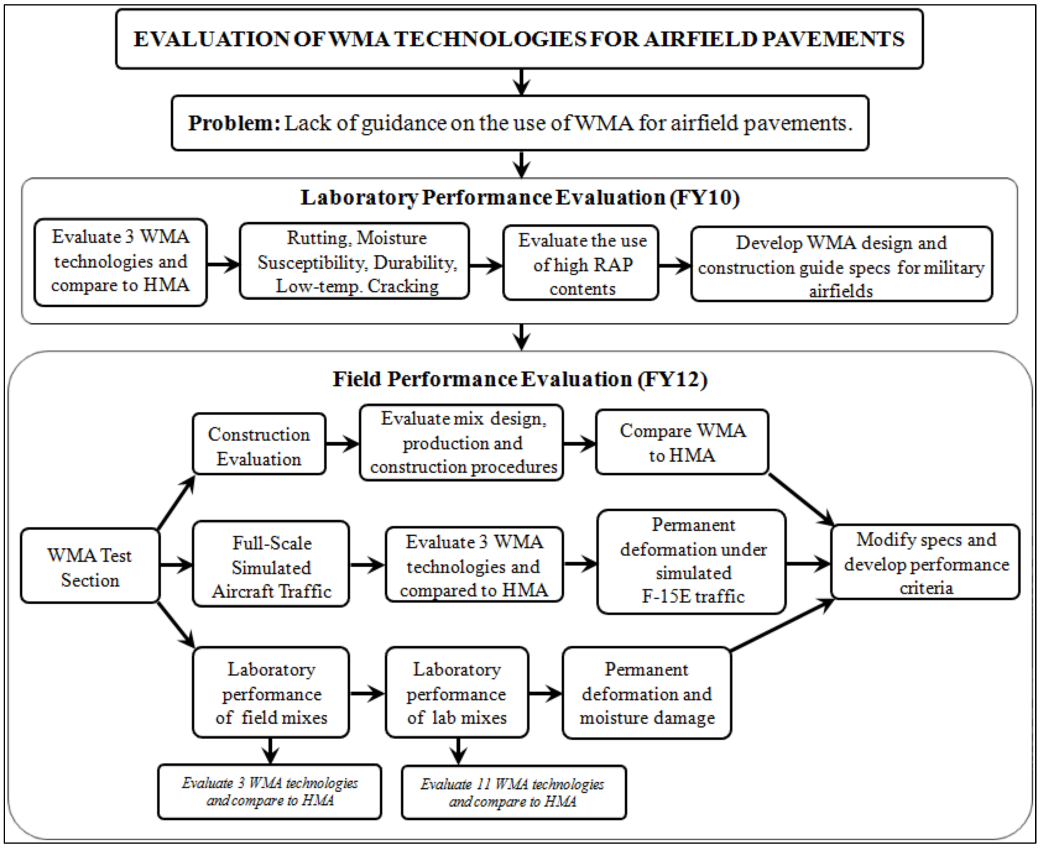


Engineering Technical Letter (ETL 11-3) were developed providing guidance on the use of WMA for airfield paving. Specific details on the WMA laboratory evaluation conducted in FY10 are presented in Mejías et al. (2012).

During 2012, the same team conducted additional research to validate the results of the laboratory performance evaluation using results from full-scale testing and from laboratory testing on plant-produced mixtures. This second study consisted of three main portions: 1) laboratory performance evaluation of field mixtures, 2) evaluation of production and construction procedures, and 3) full-scale simulated aircraft traffic evaluation. This report documents item 2) by comparing WMA production and placement to HMA production and placement.

## Objectives

The objective of this report is to present the observations made during the construction of the WMA full-scale test sections and to compare production and construction procedures for WMA and HMA.

## Approach

The approach for this portion of the study consisted of evaluating production and construction details for WMA and comparing them to similar details for conventional HMA. Data collected to quantify these factors included temperature, moisture content, time from production to laydown, and special equipment required.

# 2 Test Section Design

## General description

The test section consisted of four test items (one HMA item and three WMA items) as shown in Figure 2. The three WMAs used included one product from each of three common categories; organic waxes, chemical additives, and foaming agents. The materials used for full-scale production were selected based on local availability. Each test item was 12 ft. wide by 50 ft. long. Overrun areas at each end of the test section and a buffer zone in the middle of the test section were incorporated to facilitate construction of the asphalt concrete layers and trafficking of the test items.

Figure 2. WMA test section layout.

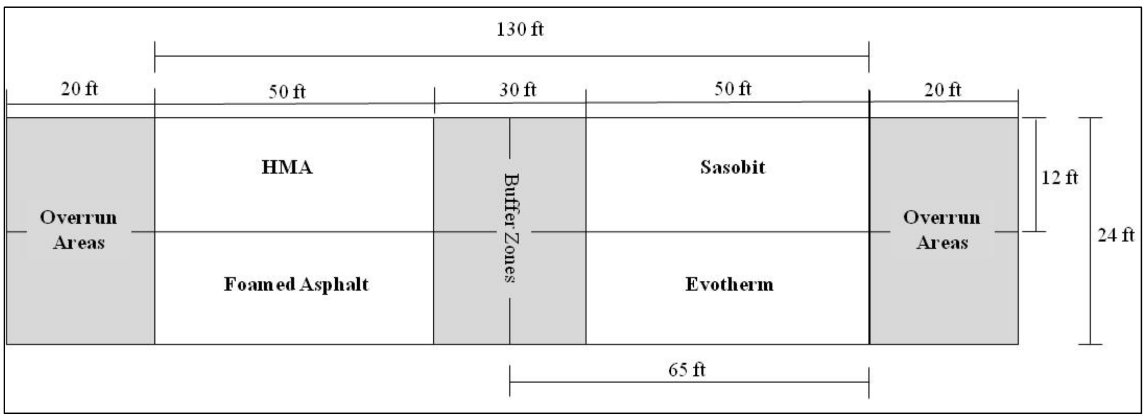


The pavement structure was designed to minimize deformation in the unbound layers so that failure would occur predominantly in the surface layer. Pavement Computer Aided Structural Evaluation (PCASE) software was used to determine the optimum pavement structural design using locally-available materials that would withstand more than 100,000 passes of a fully loaded F-15E aircraft (approximately 35-kips wheel load and 325-psi tire pressure) without failure according to Department of Defense (DoD) criteria (UFC 3-260-02) for medium-load Air Force airfields. Failure for this analysis was defined as 1 in. of rutting in the subgrade or subbase. The resulting pavement structure consisted of 4 in. of asphalt concrete over 10 in. of limestone base course with a California Bearing Ratio (CBR) of 100. The subbase layer was clay gravel with a thickness of 12 in. and a CBR of 30, placed over a high-plasticity clay subgrade with a CBR of 15. Each test item

was designed using the same pavement structure (Figure 3) with the surface course being either one of the three WMAs being evaluated or the HMA.

Figure 3. Pavement structure of the test items.

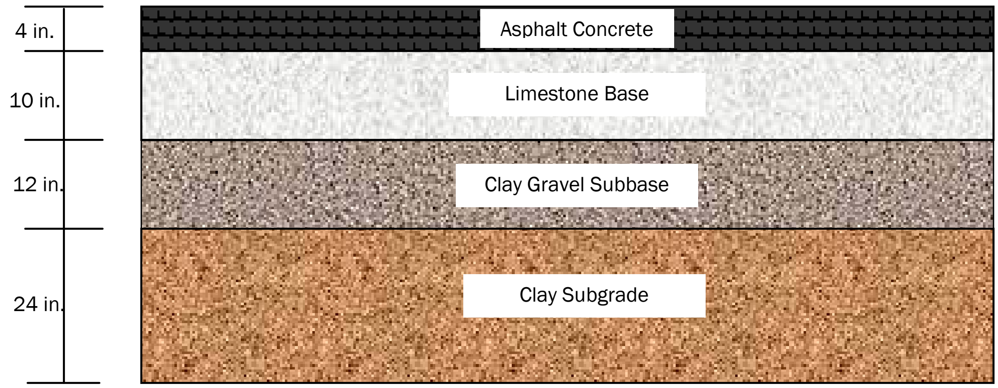


## Materials

The following sections discuss the properties of the materials used within the pavement structure based on laboratory and/or field testing. A summary of soil properties for the foundation layer described herein is given in Table 1.

Table 1. Summary of foundation layer soil properties

| | Foundation Layer | | |
|---|---|---|---|
| Material Property | Subgrade | Subbase | Base |
| Description | Buckshot Clay | Clay Gravel | Crushed Limestone |
| Color | Gray | Reddish Brown | Gray |
| USCS Group Classification | (CH) Fat Clay | (SC) Clayey-Sand with Gravel | (GP-GM) Poorly Graded Gravel with Silt & Sand |
| Liquid Limit (LL) | 77 | 29 | Non-plastic |
| Plastic Limit (PL) | 22 | 14 | Non-plastic |
| Plasticity Index (PI) | 55 | 15 | Non-plastic |
| Fines (%) | 89.9 | 13.7 | 10.0 |
| Sand (%) | 6.2 | 69.5 | 43.6 |
| Gravel (%) | 3.9 | 16.8 | 46.4 |
| Max Dry Density (pcf) | 106.2 | 130.6 | 144.7 |
| Opt. Moisture Content (%) | 19.4 | 8.0 | 4.9 |

### Clay subgrade

The subgrade consisted of a clay material classified as CH by the Unified Soil Classification System (USCS) described in ASTM D 2487. This material was procured from a local source in Vicksburg, MS and had the grain size distribution shown in Figure 4. A moisture-density relationship determined using modified Proctor compaction (ASTM D 1557) is given in Figure 5. The laboratory CBR-moisture content relationship (ASTM D 1883) is shown in Figure 6. These data were used to determine the target moisture content and dry density required to obtain the target CBR of 15. Although the laboratory CBR-moisture curve indicated the target moisture content would be 28 percent, experience with the soil has shown that the target CBR value of the field compacted material can be achieved at a moisture content of approximately 22 percent.

### Clay gravel subbase

The subbase material was a clay-gravel mixture procured from a local source in Vicksburg, MS. The USCS classification of the subbase was clayey sand (SC) with gravel. The grain size distribution of the soil is shown in Figure 7. Moisture-density and CBR-moisture content relationships are shown in Figures 8 and 9, respectively. These data were used to determine the target moisture content and dry density required to obtain the target CBR of 30. The target moisture content for the subbase was 8 percent.

Figure 4. Grain size distribution of subgrade material.

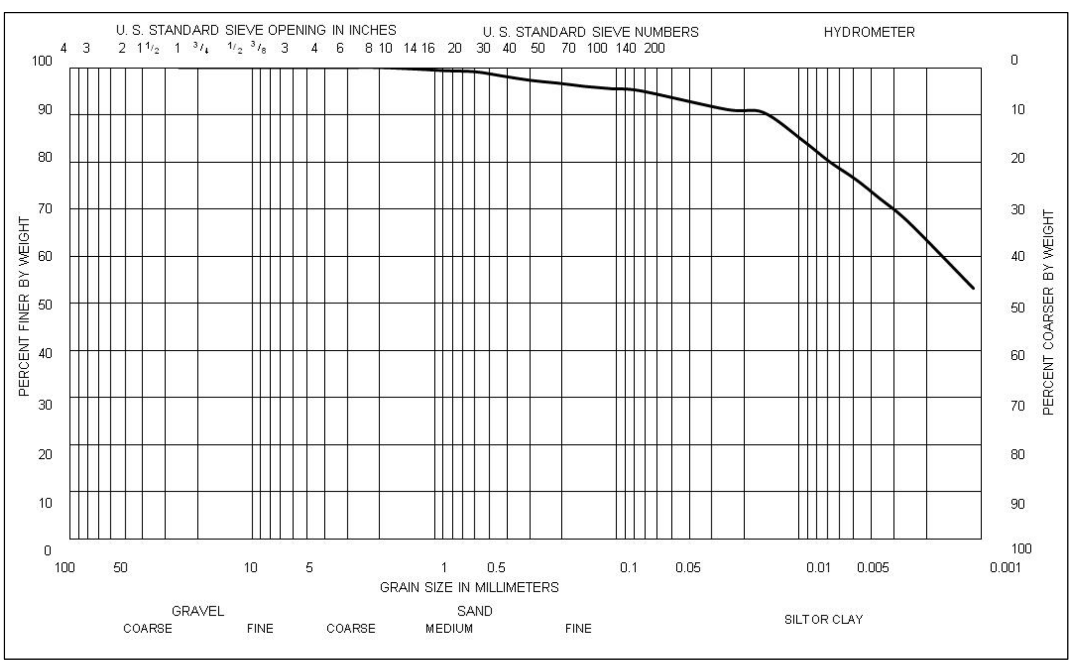

Figure 5. Dry density vs. moisture content for subgrade material.

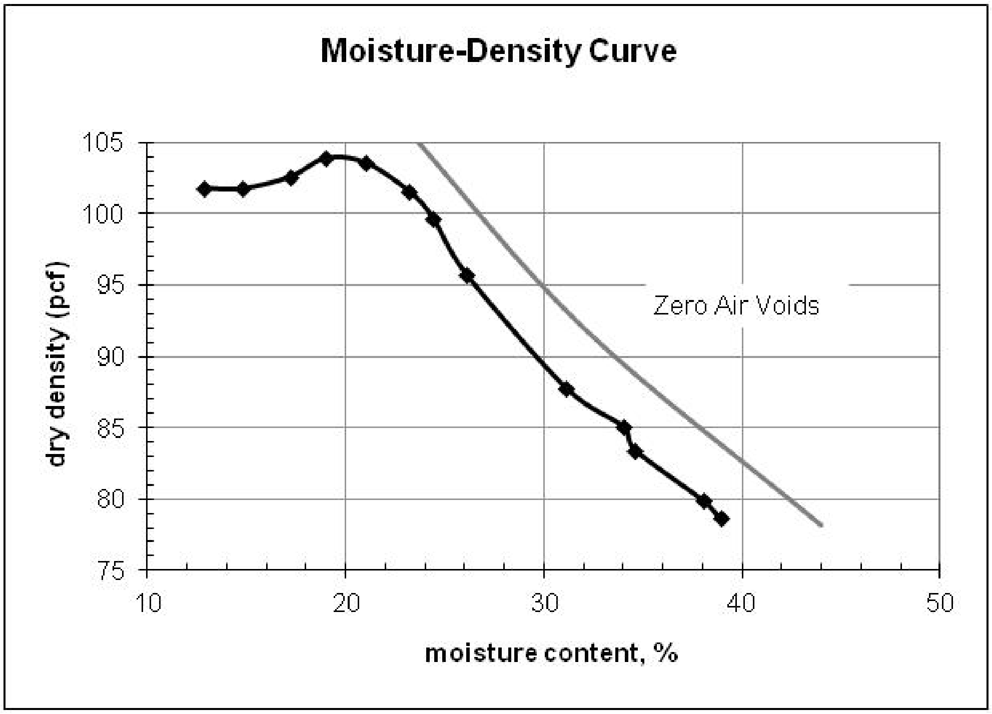


Figure 6. CBR vs. moisture content for subgrade material.

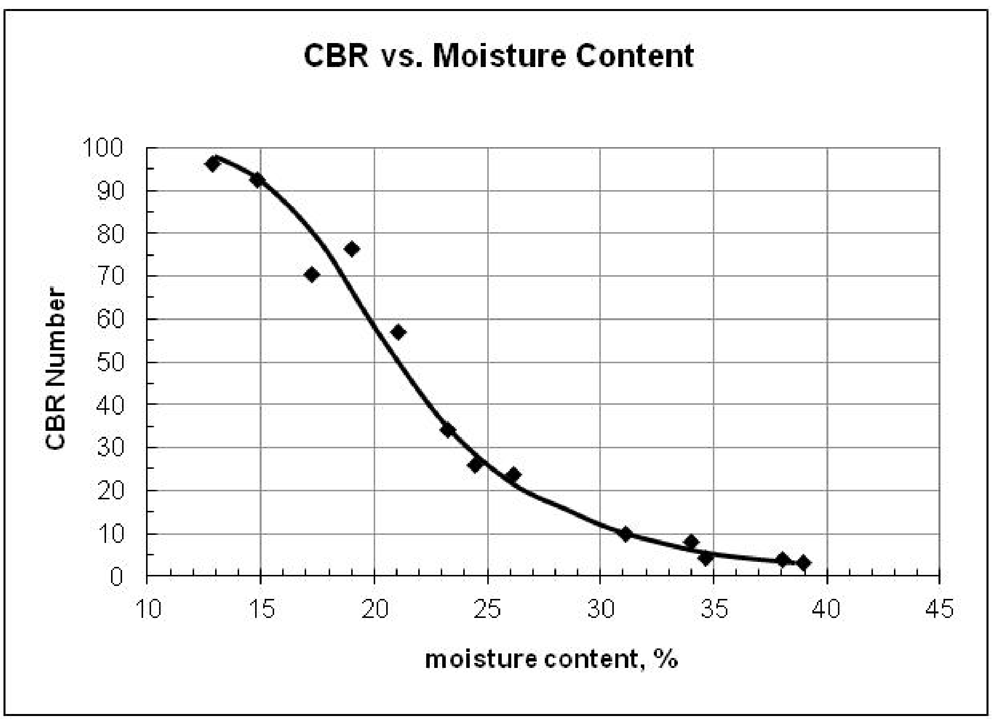

Figure 7. Grain size distribution of subbase material.

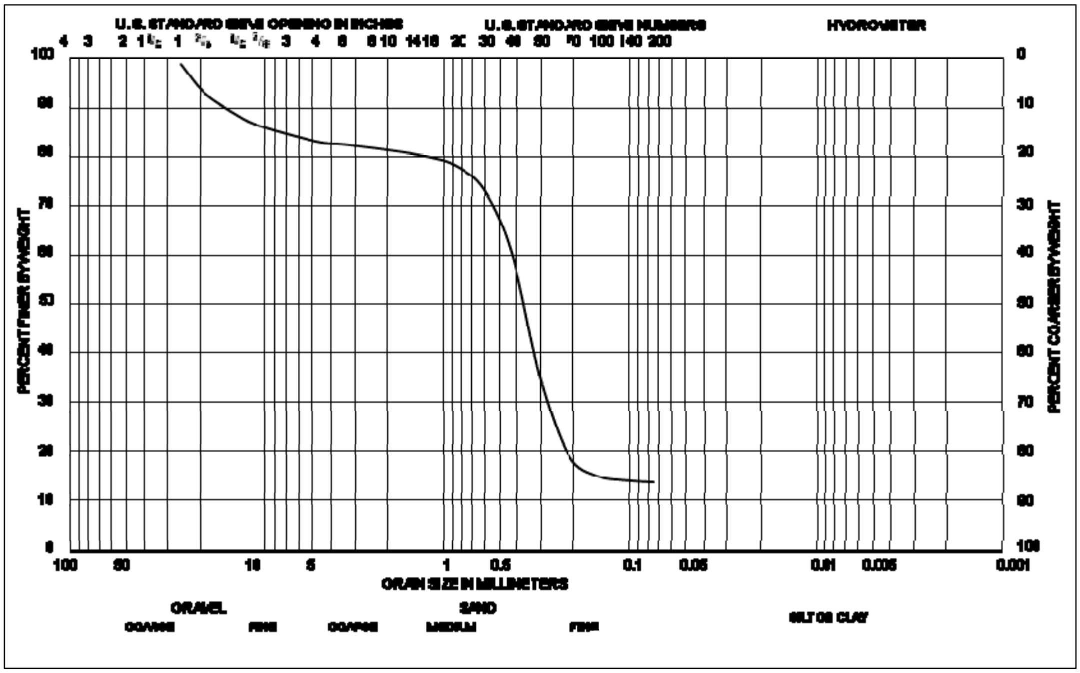


Figure 8. Dry density vs. moisture content for subbase material.

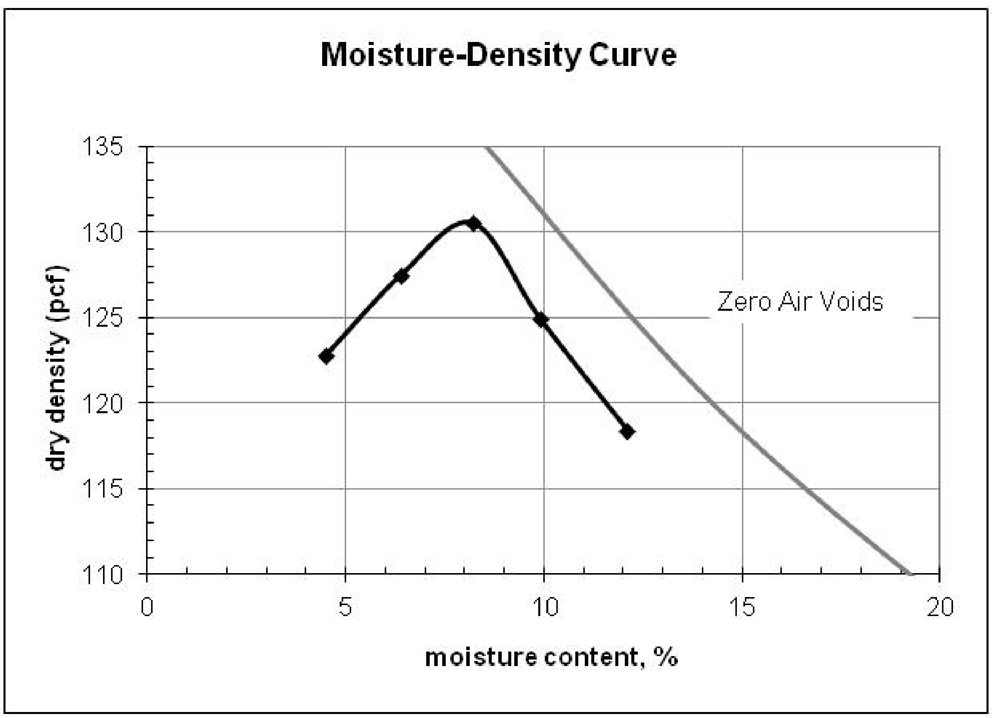

Figure 9. CBR vs. moisture content for subbase material.

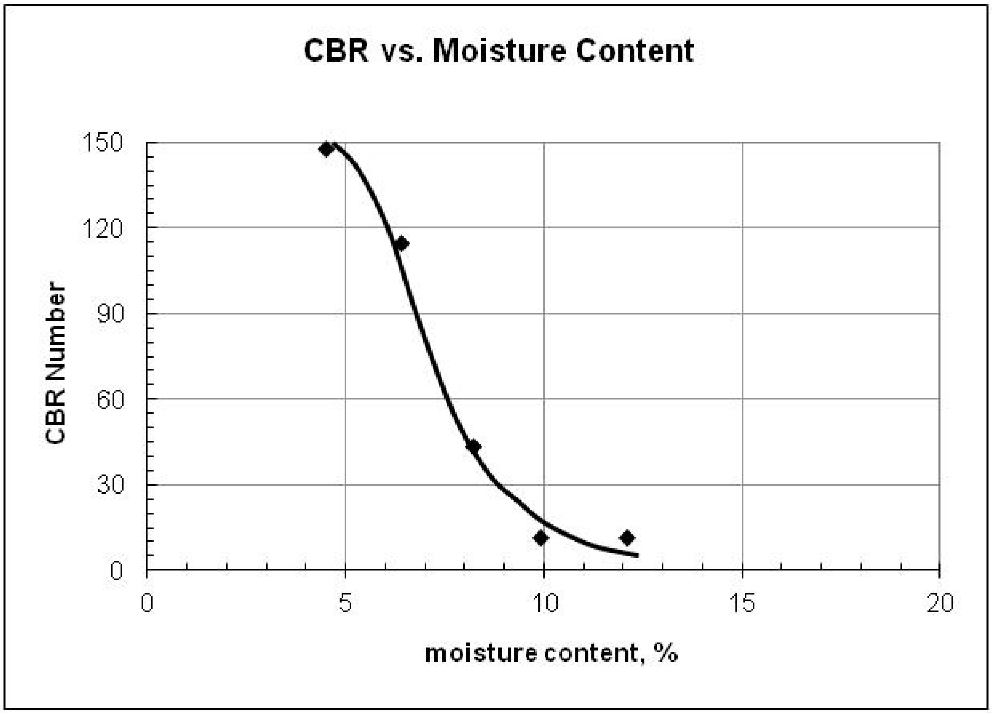


### Limestone base

The base course was a crushed limestone material stockpiled at a local facility. It was previously transported by barge to Vicksburg from its source in western Kentucky. The USCS classification of the base was gravel with silt and sand (GP-GM). The grain size distribution of the soil is shown in Figure 10. Moisture-density and CBR-moisture content relationships are shown in Figures 11 and 12, respectively. The base course had a target CBR value of 100. The desired moisture content was between 3 and 5 percent to achieve a CBR equal to, or greater than, 100.

### Soil resilient modulus testing

Additional laboratory testing was conducted with each material to determine resilient modulus ($M_R$) properties. Three replicate specimens of each soil were prepared to 98 percent of the maximum dry density at the optimum moisture content. Resilient modulus testing was then performed according to the procedure established by the National Cooperative Highway Research Project (NCHRP) 1-28A and summarized in NCHRP Research Results Digest 285. The data from this testing may be found in the appendix (Tables A1 to A9). A constitutive model based on the work of Uzan (1985) was fitted to the data (Equation 1), and Table 2 summarizes the

results. The fit of the model was very good with $R^2$ values of at least 0.95. The parameters $k_1$ and $k_3$ decreased for stronger materials while the parameter $k_2$ increased for stronger materials.

Figure 10. Grain size distribution of base material.

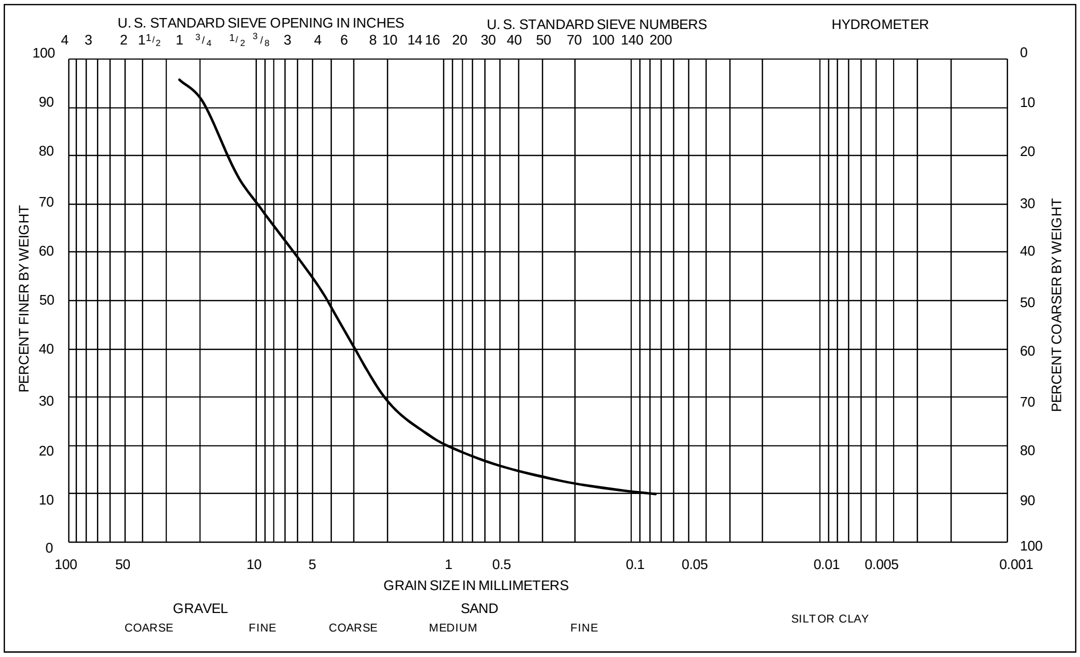


Figure 11. Dry density vs. moisture content for base material.

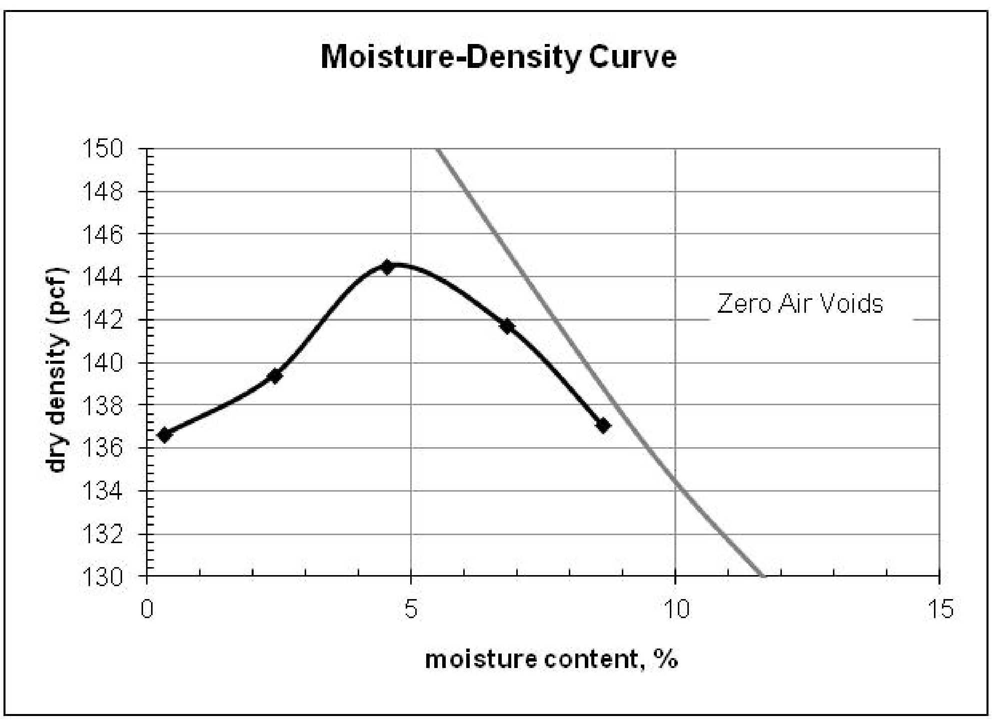

Figure 12. CBR vs. moisture content for base material.

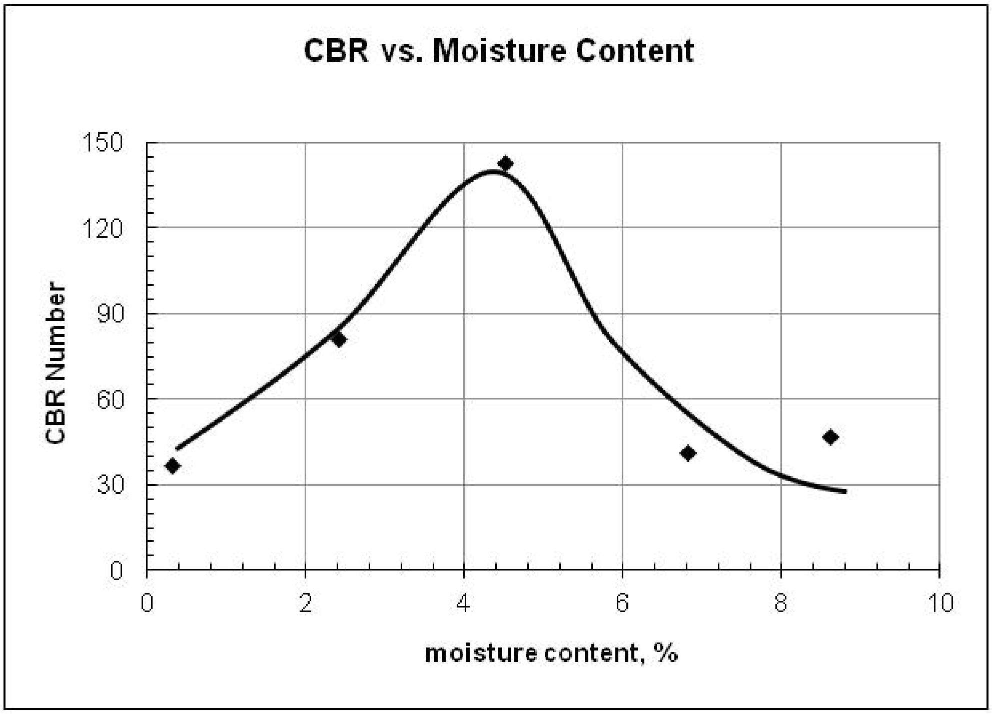


Table 2. Summary of foundation layer resilient modulus data.

| Material | Rep | $k_1$ | $k_2$ | $k_3$ | $R^2$ |
|---|---|---|---|---|---|
| Base | 1 | 1421.2 | 0.907 | -0.578 | 0.99 |
| | 2 | 1350.2 | 0.995 | -0.648 | 0.99 |
| | 3 | 1405.2 | 0.978 | -0.662 | 0.99 |
| | **Avg.** | **1392.2** | **0.960** | **-0.629** | — |
| Subbase | 1 | 1628.2 | 0.746 | -0.636 | 0.95 |
| | 2 | 1503.4 | 0.753 | -0.588 | 0.96 |
| | 3 | 1560.1 | 0.74 | -0.596 | 0.95 |
| | **Avg.** | **1563.9** | **0.746** | **-0.607** | — |
| Subgrade | 1 | 1969.4 | 0.385 | -0.319 | 0.99 |
| | 2 | 1913.9 | 0.559 | -0.414 | 0.99 |
| | 3 | 2248.5 | 0.431 | -0.371 | 0.98 |
| | **Avg.** | **2043.9** | **0.458** | **-0.368** | — |

$$M_R = k_1 P_a \left[\frac{q}{P_a}\right]^{k2} \left[\frac{t_{oct}}{P_a}\right]^{k_3} \qquad (1)$$

where

$M_R$ = resilient modulus
$P_a$ = atmospheric pressure
$\theta$ = bulk stress from (Eq 2)
$\tau_{oct}$ = octahedral shear stress from (Eq 3)
$k_1, k_2, k_3$ = material parameters from fitting the model to test data

$$\theta = \sigma_1 + \sigma_2 + \sigma_3 \tag{2}$$

$$\tau_{oct} = \frac{1}{3}\sqrt{(\sigma_1 - \sigma_2)^2 + (\sigma_1 - \sigma_3)^2 + (\sigma_2 - \sigma_3)^2} \tag{3}$$

where

$\sigma_1, \sigma_2, \sigma_3$ = principal normal stresses

### Asphalt concrete

#### *Aggregate*

An aggregate blend was designed to meet Job Mix Formula (JMF) gradation requirements for a 0.5 in. (12.5 mm) nominal maximum aggregate size mixture according to UFGS 32 12 15.13, *Hot Mix Asphalt for Airfields*. The blend consisted of 45 percent crushed gravel, 40 percent limestone, and 15 percent natural sand (maximum allowed by specification). The aggregate sources and blend were selected based on materials available for plant production. The fine aggregate angularity (FAA) value for this blend of 42.6 percent was below specified minimum requirements of 45.0 percent and could indicate increased propensity for rutting. Gradation and aggregate properties for the JMF aggregate blend are provided in Figure 13.

#### *Binder and WMA additives*

The base binder used for this project was an unmodified PG 67-22. A neat asphalt binder was used instead of a polymer-modified binder to avoid any interaction between WMA technologies and other binder modifiers. The Evotherm™ additive was pre-blended with the base binder at the asphalt terminal prior to use. Evotherm™ is a commonly used, proprietary chemical additive that produces WMA by reducing the binder's viscosity. The addition of Sasobit® additive and water injection to produce foamed asphalt was performed at the asphalt plant. Sasobit® is an organic hydrocarbon based wax manufactured by Sasol Wax GmbH. Above its melting point of 100 °C (212 °F), Sasobit® reduces the measured asphalt viscosity which

Figure 13. Gradation and properties of aggregate for asphalt mixtures.

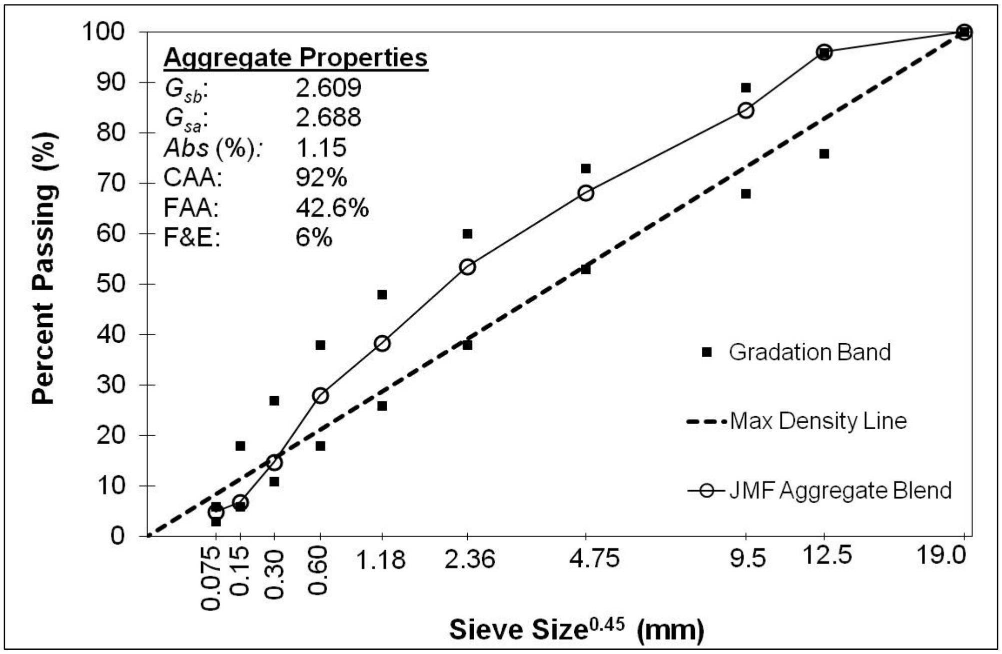


permits reduction of the mix temperature and promotes asphalt mixing and compaction. Below its melting point Sasobit® solidifies into a lattice structure that stiffens the asphalt binder. The foamed asphalt used water injection near the binder feed line. Foamed asphalt caused by the vaporization of water reduces binder viscosity and promotes mixing. The specific dosage rates and detailed product descriptions are provided in Doyle et al. (in preparation).

*Mix design*

Asphalt mixtures were designed to 75 gyrations in the Superpave Gyratory Compactor (SGC) according to UFGS 32 12 15.13 requirements. The design binder content was selected as the binder content that resulted in a compacted specimen having 4.0 percent air voids. Theoretical maximum specific gravity ($G_{mm}$) of each mixture was determined on duplicate specimens and averaged according to American Association of State Highway and Transportation Officials (AASHTO) T 209. Bulk specific gravity ($G_{mb}$) of compacted cylindrical specimens was determined according to AASHTO T 331 and used to determine specimen air voids ($V_a$). Specific details about the mix designs are given in Doyle et al. (in preparation).

# 3 Test Section Construction

A full-scale test section consisting of four individual, instrumented test items was constructed under shelter in the Hangar 4 pavement test facility at ERDC to provide a thorough comparison of constructing WMA pavement versus HMA pavement. The following paragraphs describe the construction of the full-scale test section.

## General description

A 30-ft.-wide by 170-ft.-long test pit was excavated to a minimum 48-in.-depth below the existing finished grade in Hangar 4, as shown in Figure 14, to construct the pavement structure. The 4-in.-thick asphalt concrete surface layers were placed on top of a 10-in.-thick crushed limestone base, a 12-in.-thick clay-gravel subbase, and a 24-in.-thick high-plasticity clay subgrade constructed to a CBR of 15 over an existing silt foundation, as shown in Figure 3. Each individual test item was 12-ft.- wide by 50-ft.-long.

Figure 14. Excavating soil for test section construction.

## Subgrade construction

The 24-in.-thick compacted subgrade was constructed above the soil at the bottom of the excavation, which was a low-plasticity silt material (ML) having a CBR less than 20.The existing ML material was leveled with a bulldozer and compacted with a pneumatic-tired roller and a vibratory compactor to ensure that the remainder of the test section was constructed over a stable foundation. The bottom and sides of the test pit were lined with impervious 6-mil polyethylene sheeting to minimize moisture migration from the new soil serving as the test section subgrade.

The CH was processed at a nearby preparatory site by spreading the material to a uniform 12-in. depth, pulverizing the material with a rotary mixer, adjusting the moisture content, pulverizing the material again, and stockpiling it as shown in Figure 15. This was an iterative process necessary to achieve a uniform distribution of moisture throughout the material. Once the CH had been processed to the target moisture content, the material was spread by a bulldozer in 8-in.-thick lifts and compacted with a pneumatic-tired roller, as shown in Figure 16, to a compacted lift thickness of 6 in. A rotary mixer was used to scarify the surface between lifts to ensure good bond, as shown in Figure 17. Final grade was established using a motor grader, as shown in Figure 18. The surface was rolled smooth using a steel-wheel roller, as shown in Figure 19. CBR, moisture, and density tests were performed on each lift to measure in-situ properties.

Figure 15. Processing subgrade soil to adjust moisture content.

Figure 16. Compacting subgrade with pneumatic-tired roller.

Figure 17. Scarifying surface of subgrade lift to achieve bond between layers.

Figure 18. Establishing final grade of subgrade surface.

Figure 19. Smoothing surface of subgrade with steel-wheeled compactor.

## Subbase construction

The subbase soil was constructed over the compacted subgrade in two, 6-in.-thick lifts. The soil was processed at a nearby preparatory site using a

rotary mixer to adjust the moisture content to the desired percentage. The processed material was spread by a bulldozer (Figure 20) in 8-in.-thick lifts and compacted with a pneumatic-tired roller to a compacted lift thickness of 6 in. A motor grader was used to achieve proper grade. The surface was rolled smooth using a steel-wheel roller. CBR, moisture, and density tests were performed on each lift to measure in-situ properties.

Figure 20. Spreading subbase soil with bulldozer.

## Base construction

The base course soil was constructed over the compacted subbase in two, 5-in. lifts. The stockpiled material was spread by a bulldozer (Figure 21) in 6-in. lifts. A motor grader was used to achieve proper grade (Figure 22). The material was compacted with a pneumatic-tired roller (Figure 23) to a compacted lift thickness of 5 in. The surface was rolled smooth using a steel-wheel roller (Figure 24). CBR, moisture, and density tests were performed on each lift to measure in-situ properties.

## Soil field testing

Each foundation layer underwent a series of in situ tests to characterize the material properties in the pavement structure. The tests included CBR, nuclear density, nuclear moisture, and oven moisture. CBR characterizes the strength of each layer in the test section. Moisture and density tests

ensure the construction complies with design specifications. The following paragraphs give a description of each in situ test used during test section construction.

Figure 21. Spreading base material using a bulldozer.

Figure 22. Grading base course surface.

Figure 23. Compacting base course with pneumatic roller.

Figure 24. Final compaction of base course using steel-drum roller.

## California Bearing Ratio

In situ CBR tests (Figure 25) were conducted according to ASTM D4429 at three transverse locations at stations 15, 25, and 35 ft from the beginning

of each item for each underlying layer to determine the condition of the soil at the time of testing. The transverse locations included tests on the center-line, approximately 1 ft west of the center-line, and approximately 1 ft east of the center-line.

Figure 25. In situ CBR test.

CBR tests were mainly designed for subgrade and subbase material but can be completed on base course materials (ASTM International 2004). Also, it is important to note that CBR tests indicate the strength of the soil at the time of testing. If, for example, the moisture content changes after a CBR test, the strength of the soil (CBR) will likely also change.

### Nuclear gauge

A Troxler nuclear moisture-density gauge Model 3430 was used throughout construction to rapidly measure each layer's respective moisture content and wet and dry density. The direct method of measurement procedure detailed in ASTM D 6938 was used during field testing. Nuclear gauge measurements were used for quality control testing during construction. However, nuclear gauge results were not reported, since oven moisture contents, sand cone, and drive cylinder density values were also measured and are considered to be more reliable.

### Oven moisture

Each compacted lift in each of the foundation layers was also tested using convection oven moisture determination tests to verify that target values had been achieved. This test is performed by sampling small portions of the in situ material and drying them in an oven. The mass before and after drying is used to calculate moisture content. For this project, samples were obtained immediately after CBR tests were completed. The detailed procedure can be found in ASTM D 4643.

### Sand cone density

Soil density was measured using the sand cone method for the base and subbase layers as shown in Figure 26. The sand cone test is performed by excavating a small amount of soil and replacing it with a standard sand material. The volume of sand required to fill the excavation is determined. The in-situ density is calculated based on the mass of the soil and the measured volume of sand required to fill the hole. The detailed procedure can be found in ASTM D 1556.

### Drive cylinder density

Density of the subgrade was measured using the drive cylinder method following ASTM D 2937 guidance. The procedure involves driving a canister into a fine-grained soil (Figure 27). The canister is then excavated using a shovel or other tool. Excess soil from around the canister is removed. The mass of the soil in the canister is divided by the known volume to determine in-situ density. Results from oven moisture, sand cone density, and drive cylinder density tests are given in Table 3.

## Asphalt concrete paving

The asphalt was produced by APAC Mississippi, Inc. from a local drum mix plant in Vicksburg, MS and delivered to the construction facility. Approximately 15 tons from the beginning of each mixture were wasted to ensure a uniform material was produced in the plant. The asphalt mixture was delivered to the Hangar 4 facility to place within an hour of mixing; no material was stored in the silo for an extended period of time. Aggregate samples were collected from the plant's feed belts (Figure 28) to verify properties. Samples of the mixtures were collected from elevated platforms at the plant (Figure 29) to verify that the mix design had been achieved.

Figure 26. Performing density tests on compacted subbase using sand cone method.

Figure 27. Drive cylinder.

Table 3. Foundation layer properties as constructed.

| Test Item | Subgrade | | | Subbase | | | Base | | |
|---|---|---|---|---|---|---|---|---|---|
| | | Drive Cylinder | | | Sand Cone | | | Sand Cone | |
| | Avg. CBR (%) | Dry Density (pcf) | Moisture Content (%) | Avg. CBR (%) | Dry Density (pcf) | Moisture Content (%) | Avg. CBR (%) | Dry Density (pcf) | Moisture Content (%) |
| HMA | 13.8 | 97.1 | 22.8 | 26.7 | 127.7 | 8.4 | 100 | 144.3 | 2.7 |
| Foam | 15.1 | 96.2 | 21.8 | 34.6 | 130.8 | 7.5 | 106.1 | 139.7 | 2.5 |
| Sasobit® | 14.9 | 96.1 | 22.2 | 35.1 | 131.6 | 7.1 | 103.6 | 133.5 | 2.2 |
| Evotherm™ | 14.9 | 99.9 | 20.5 | 33.3 | 129.4 | 6.9 | 103.1 | 138.7 | 2.5 |
| Overall Average | 14.7 | 97.3 | 21.8 | 32.4 | 129.9 | 7.4 | 103.2 | 139.1 | 2.5 |
| Target Values | 15 | 103 | 22 | 30 | 130 | 8 | 100 | 141-145 | 3-5 |

The Evotherm™ product was pre-blended with the binder and sourced from a tanker truck. The Sasobit® and foam WMA technologies required modifications to the asphalt plant, as the plant was not configured to use these technologies. Figure 30 shows the external units used to supply the Sasobit® and foam installed according to manufacturer specifications. Figure 31 shows the connections to the drum at the plant. Target production temperatures for the HMA and WMAs, respectively, were 290°F (143°C) and 265°F (129°C).

Figure 28. Sampling aggregate from feed belt at asphalt plant.

The asphalt concrete pavement layers were constructed on the prepared base course using conventional paving equipment in two, 2-in.-thick lifts. Paving was accomplished using a Caterpillar AP655D asphalt paver (Figure 32). Breakdown rolling was performed using a Caterpillar CB-534D XW vibratory steel-wheel asphalt compactor (Figure 33). An Ingersol Rand PT125R pneumatic roller was used for intermediate rolling (Figure 34). The steel-drum roller with no vibration was used for finish rolling (Figure 35). A CRS-2 asphalt emulsion tack coat was applied between lifts.

## Surface grinding

The compacted asphalt concrete surface was surveyed to determine the total layer thickness. A uniform layer depth was desired to eliminate any effects of asphalt layer thickness on rutting performance. The thinnest pavement

Figure 29. Sampling asphalt mixture from delivery trucks.

Figure 30. External equipment required for foamed asphalt and Sasobit® WMA.

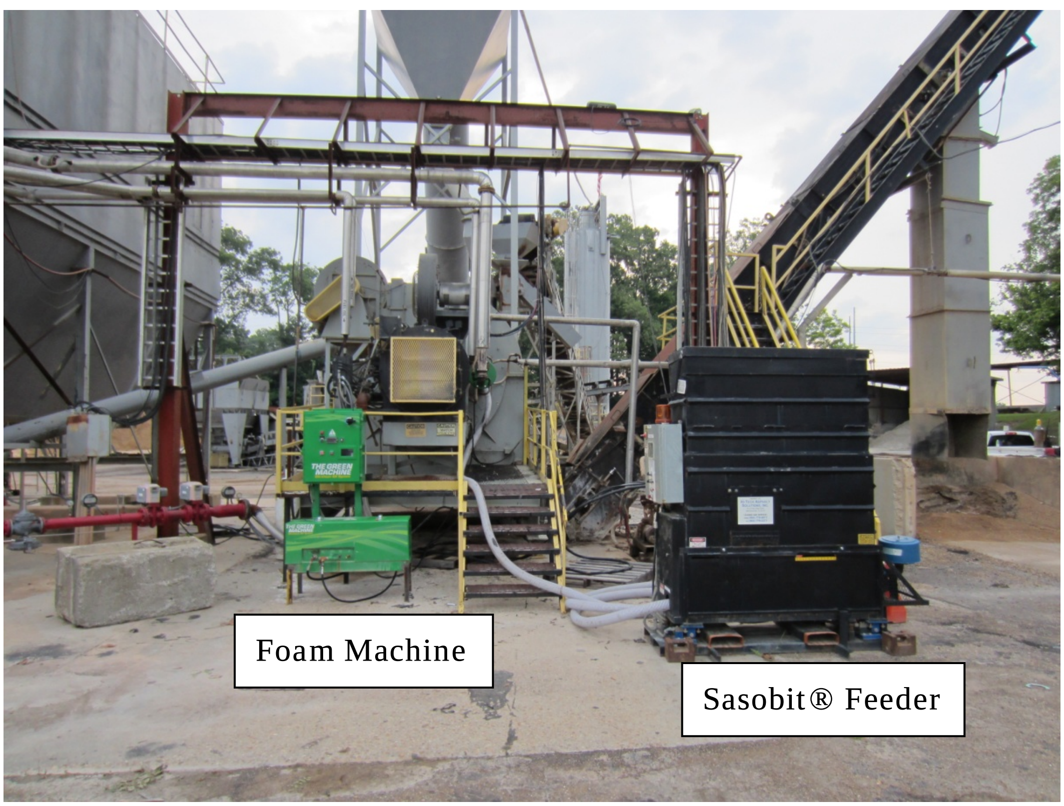

Figure 31. Attachments for WMA additives on asphalt mixing drum.

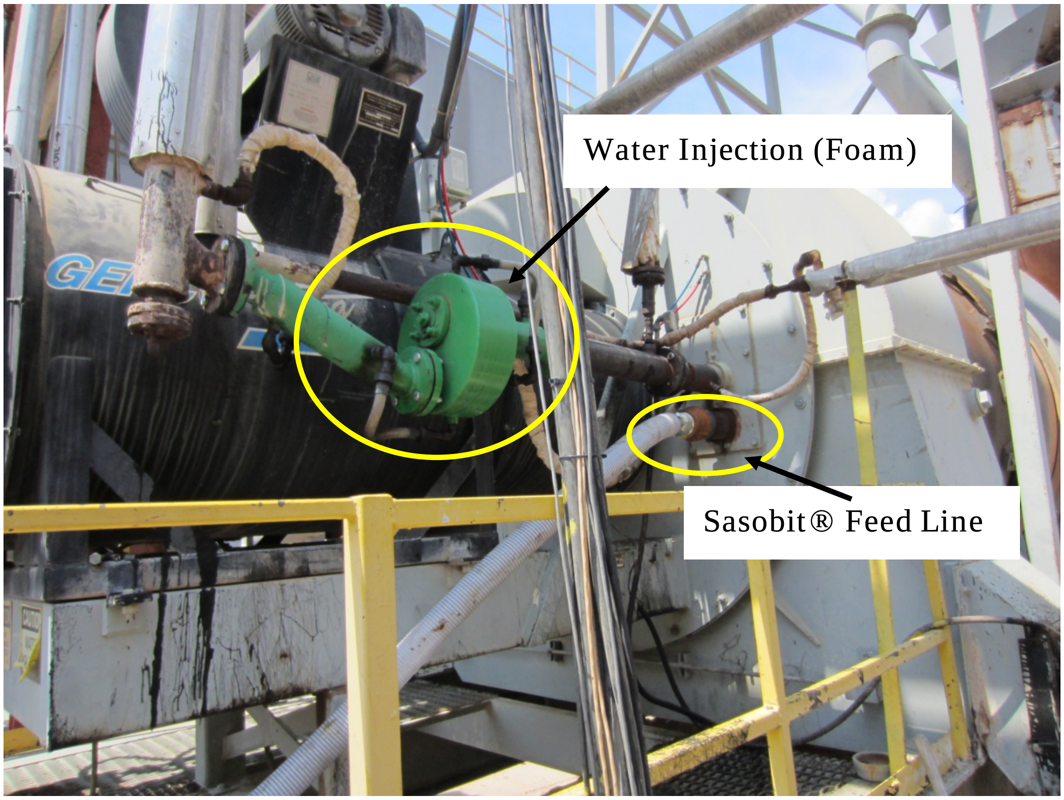


Figure 32. Paving asphalt mixture in covered test facility.

Figure 33. Breakdown rolling of asphalt concrete using vibratory compactor.

Figure 34. Intermediate rolling of asphalt concrete using pneumatic-tired roller.

Figure 35. Finish rolling asphalt concrete using static steel-wheel compactor.


area was selected as the target thickness. Any other areas thicker than this target were subjected to diamond surface grinding (Figure 36) to reduce the thickness of the asphalt concrete layer. Surface grinding removes thin layers from the pavement surface and is commonly used to correct grade deficiencies or roughness. Figure 37 shows the surface of a pavement area after diamond grinding.

Figure 36. Surface grinding to create uniform asphalt thickness.

Figure 37. Pavement surface after grinding.

## Survey data

Robotic total station recordings of elevation, as well as northing and easting, were collected before and after each pavement layer was constructed to verify total thickness. Measurements were taken along the center-line of each item at 1-ft. intervals. Measurements were also taken at 1-ft. intervals transversely across each item at stations 15, 25, and 35 ft from STA 0+00 of the center-line. These locations are referred to as “cross-section” in this report. Figures 38 through 53 provide designed and surveyed elevation data for each item.

During construction, the location of instrumentation was also surveyed for elevation to ensure placement at the proper location. Locations of earth pressure cells (EPC), single depth deflectometers (SDD), and asphalt strain gauges (ASG) are indicated by symbols denoted on the figures. Further descriptions of the instrumentation are provided in the next section of this report. Table 4 summarizes the as-constructed layer thicknesses for each test item. In general, pavement layers were constructed at elevations and to thicknesses very close to the design.

Figure 38. HMA center-line layer thicknesses as constructed.

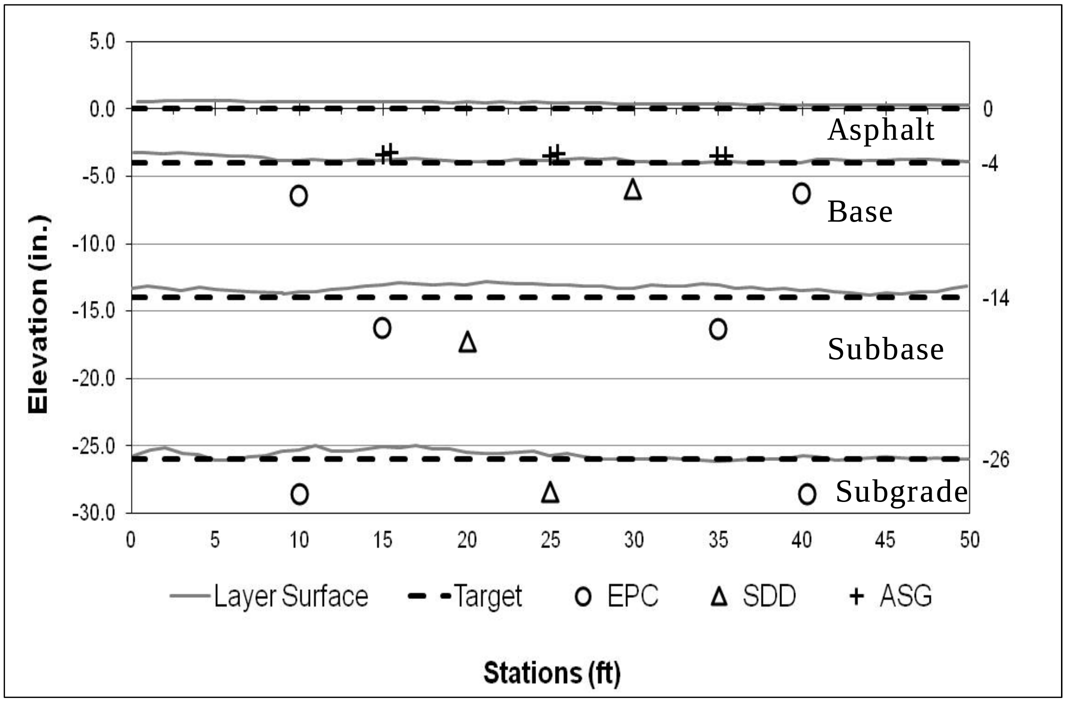


Figure 39. HMA STA 0+15 cross-section layer thicknesses as constructed.

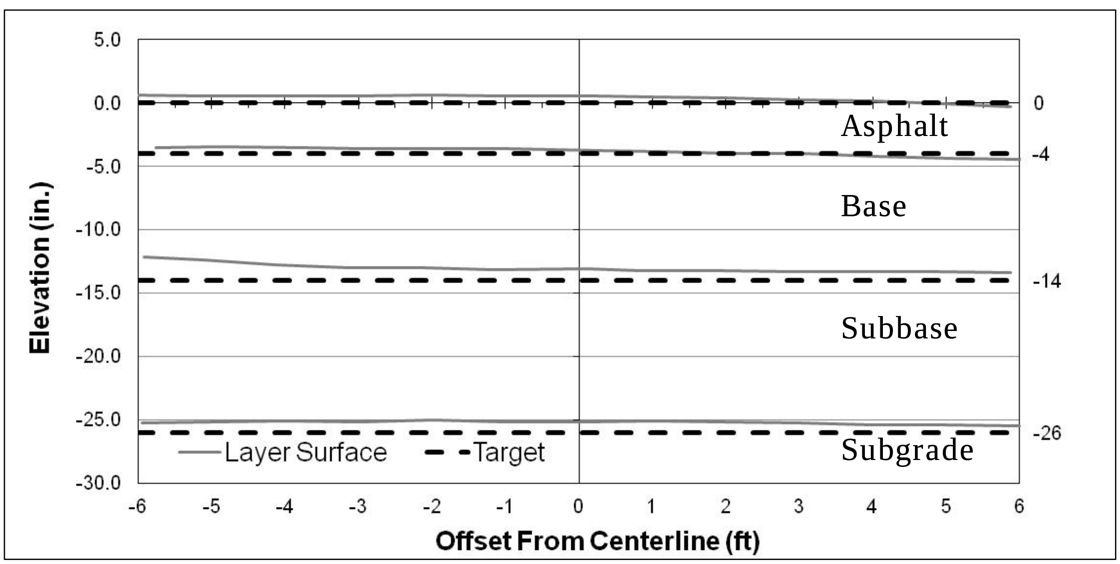

Figure 40. HMA STA 0+25 cross-section layer thicknesses as constructed.

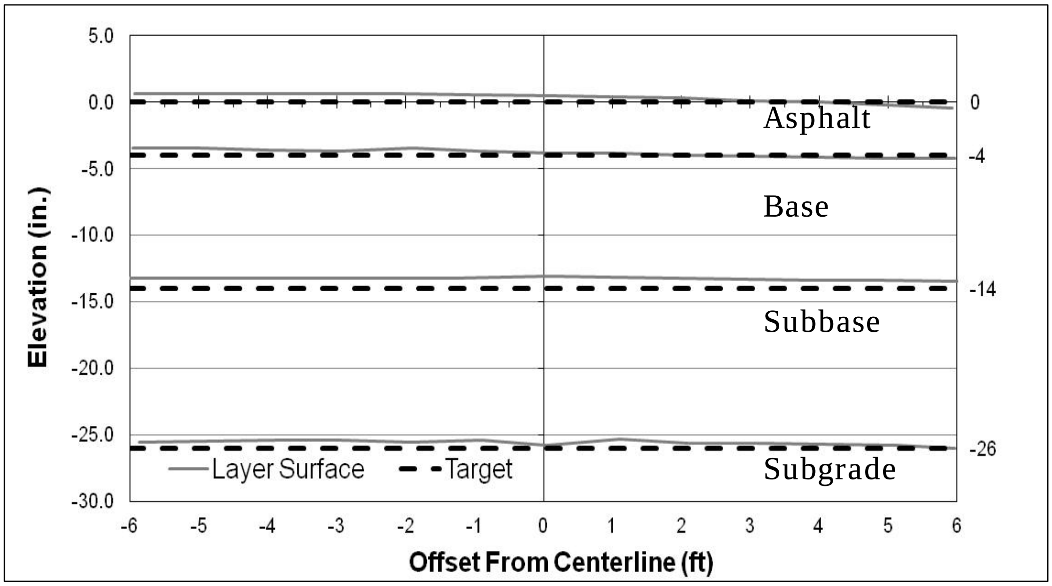


Figure 41. HMA STA 0+35 cross-section layer thicknesses as constructed.

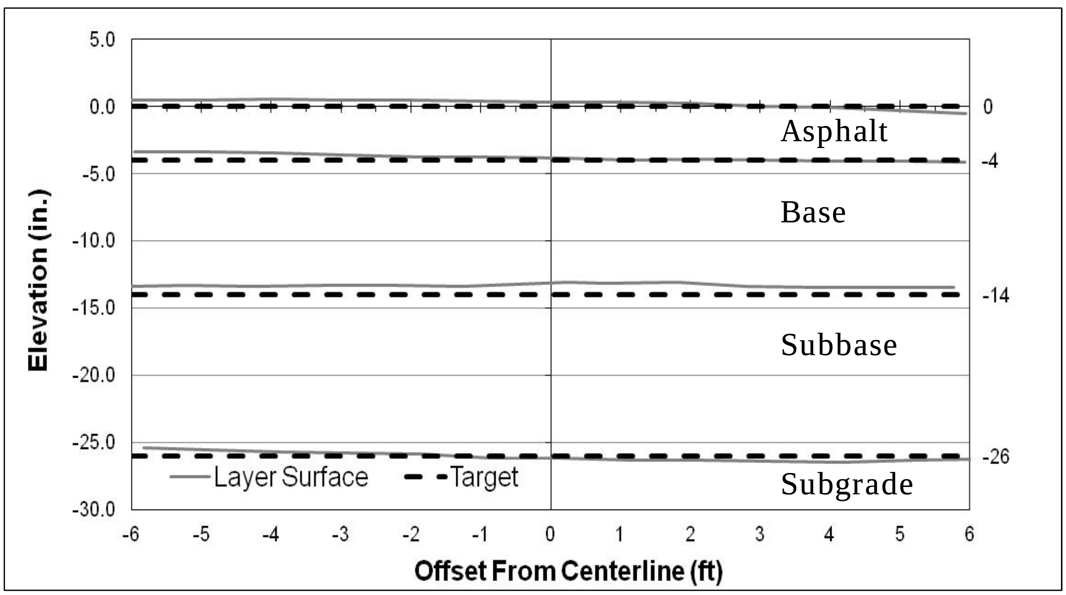

Figure 42. Foamed asphalt center-line layer thicknesses as constructed.

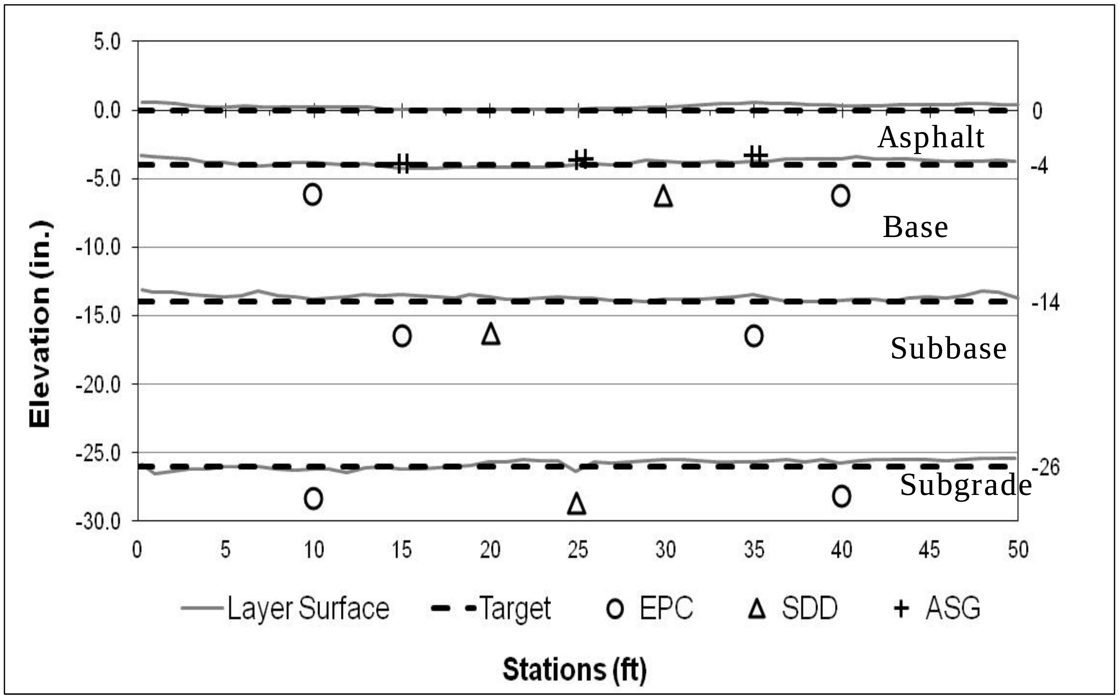


Figure 43. Foamed asphalt STA 0+15 cross-section layer thicknesses as constructed.

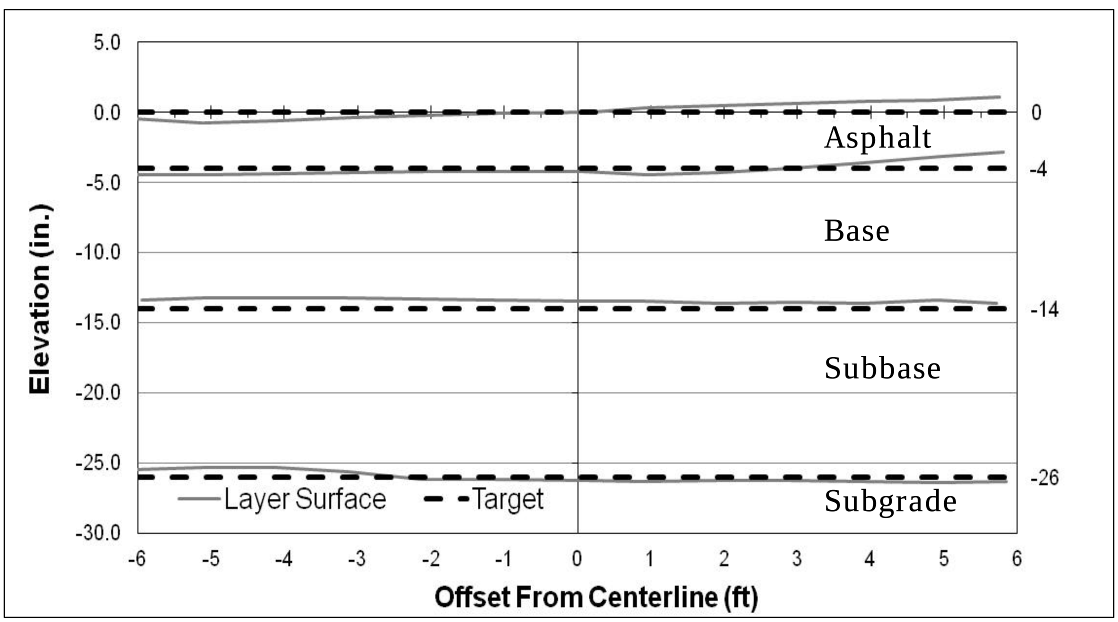

Figure 44. Foamed asphalt STA 0+25 cross-section layer thicknesses as constructed.

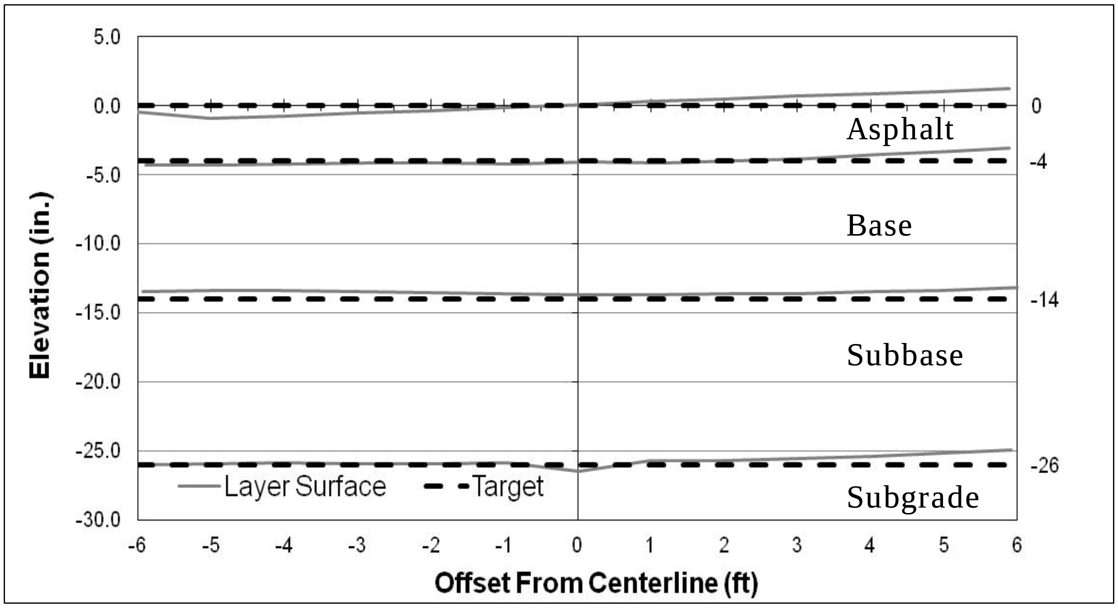


Figure 45. Foamed asphalt STA 0+35 cross-section layer thicknesses as constructed.

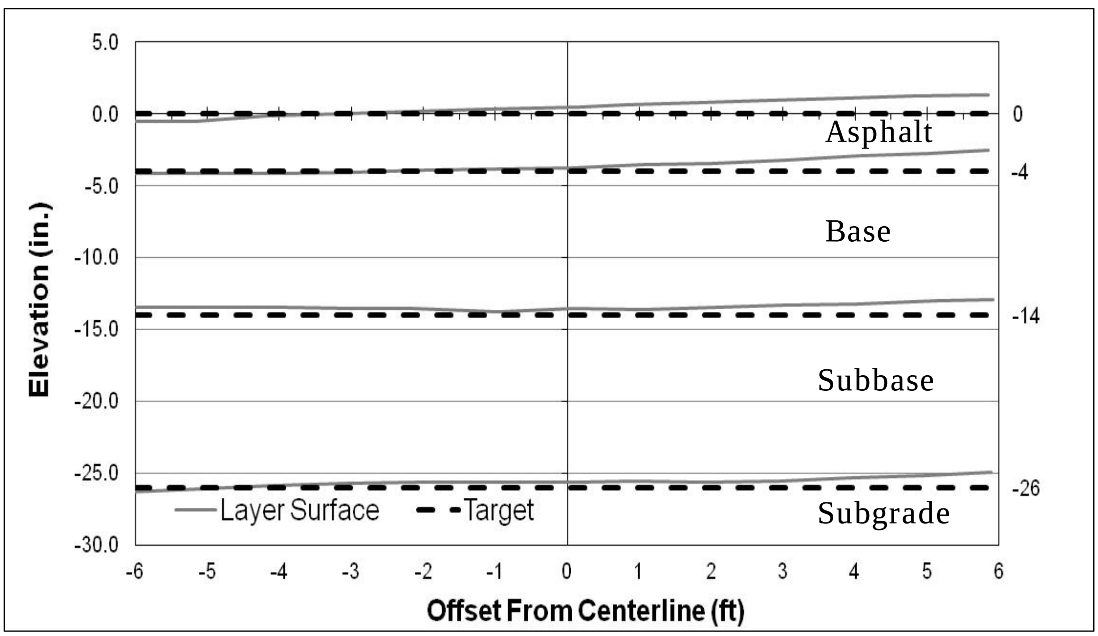

Figure 46. Sasobit® center-line layer thicknesses as constructed.

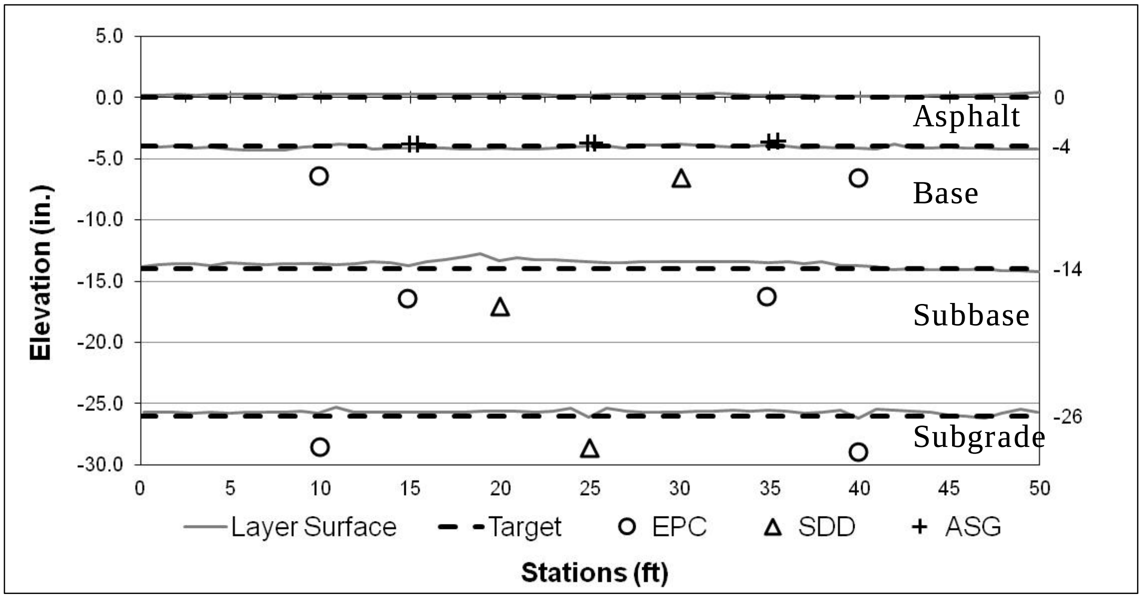


Figure 47. Sasobit® STA 0+15 cross-section layer thicknesses as constructed.

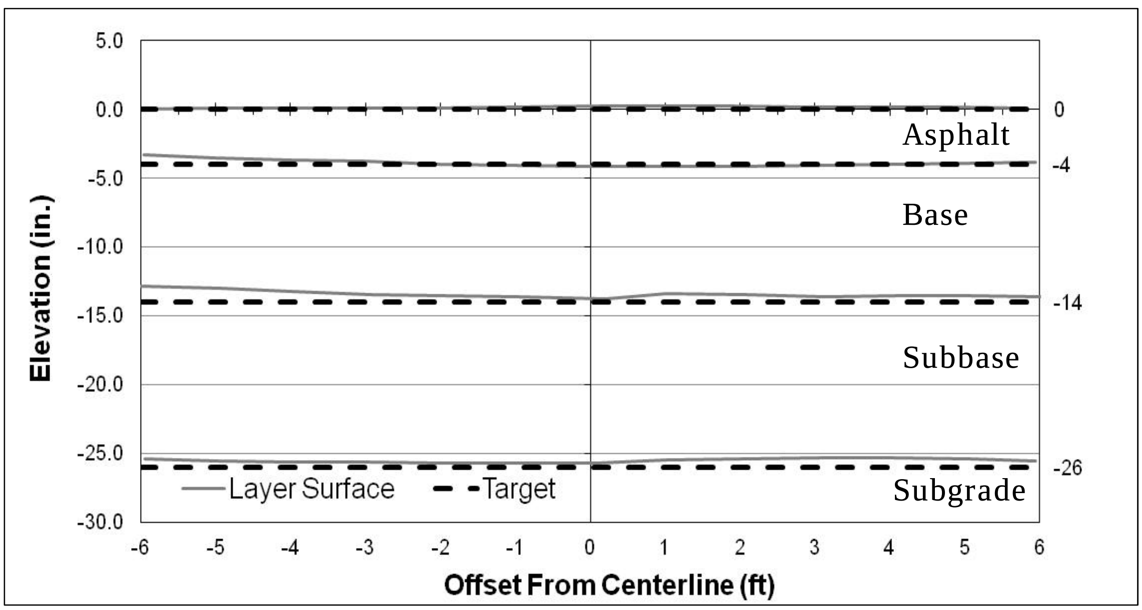

Figure 48. Sasobit® STA 0+25 cross-section layer thicknesses as constructed.

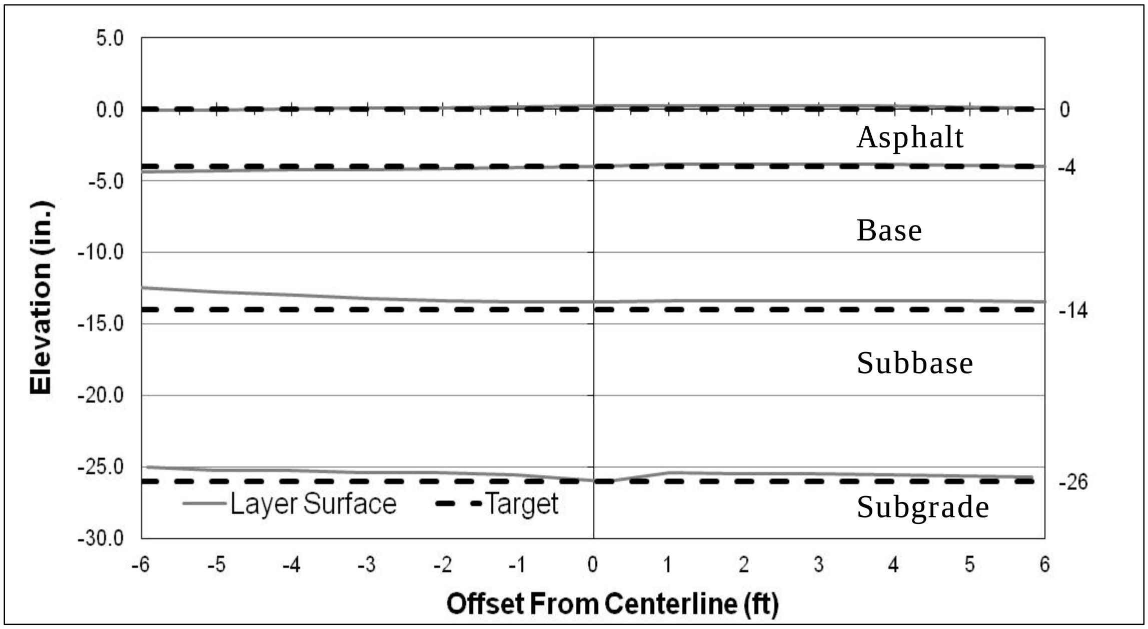


Figure 49. Sasobit® STA 0+35 cross-section layer thicknesses as constructed.

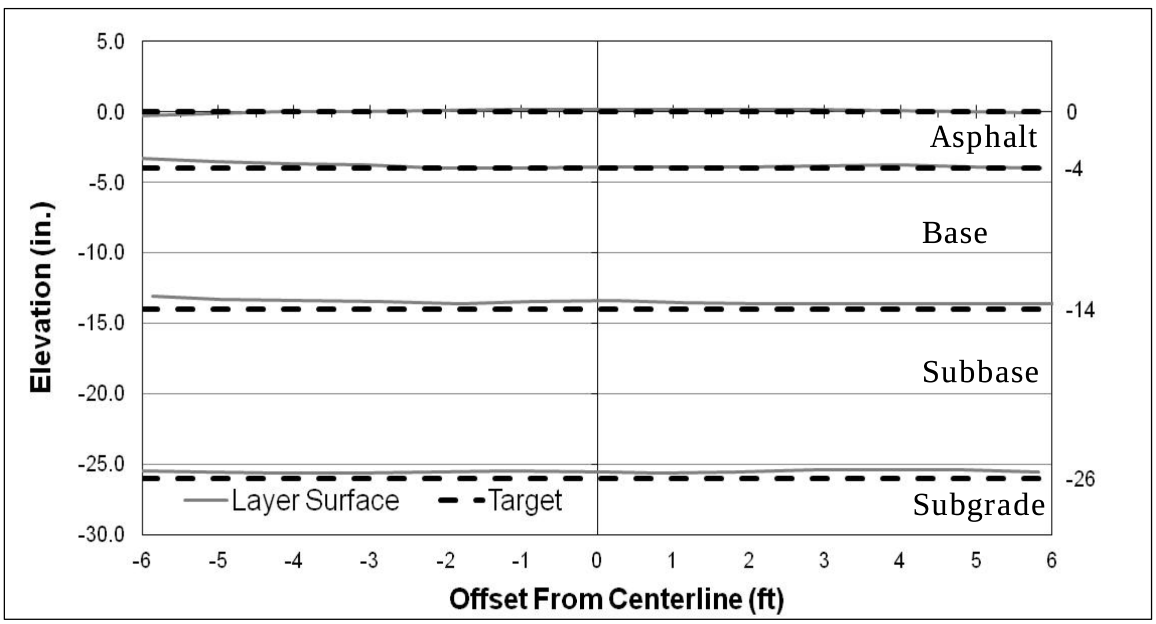

Figure 50. Evotherm™ center-line layer thicknesses as constructed.

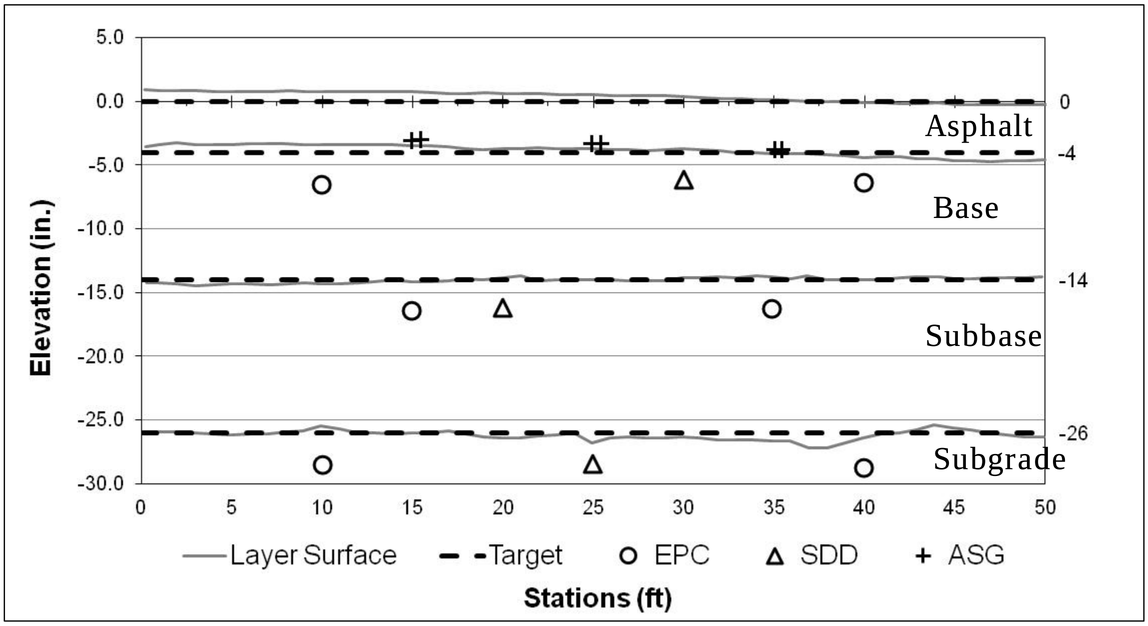


Figure 51. Evotherm™ STA 0+15 cross-section layer thicknesses as constructed.

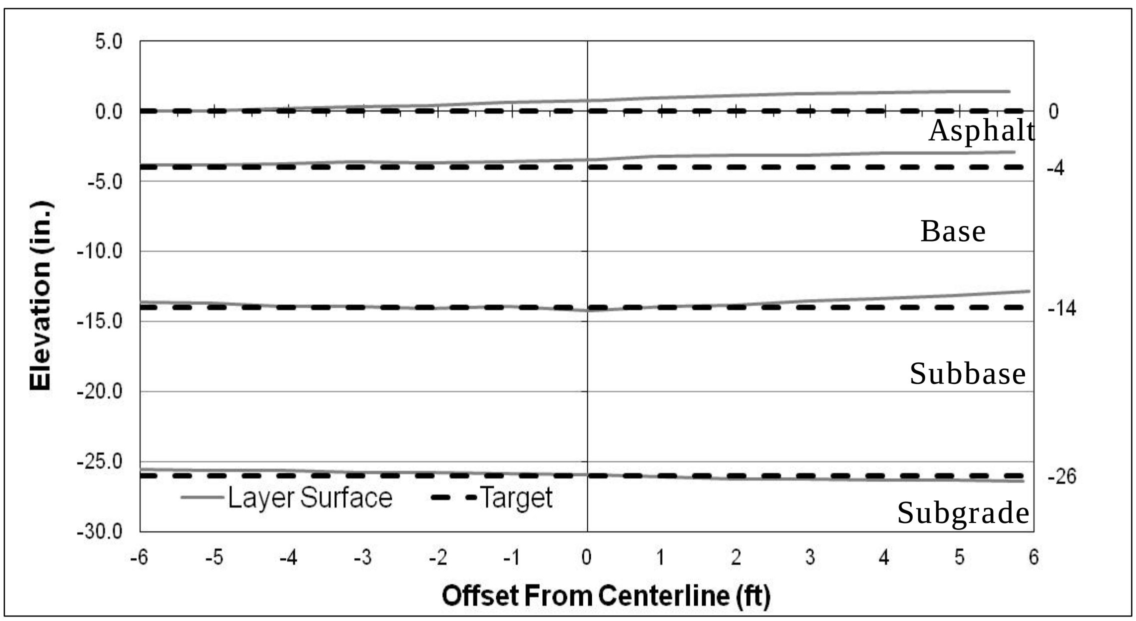

Figure 52. Evotherm™ STA 0+25 cross-section layer thicknesses as constructed.

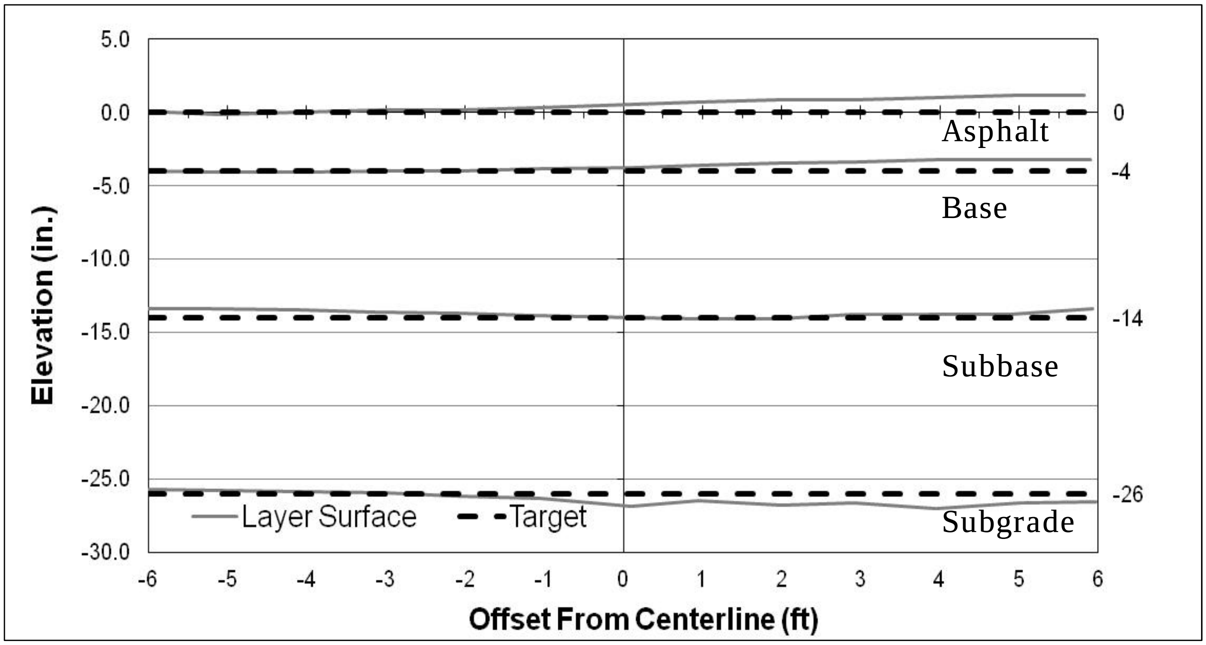


Figure 53. Evotherm™ STA 0+35 cross-section layer thicknesses as constructed.

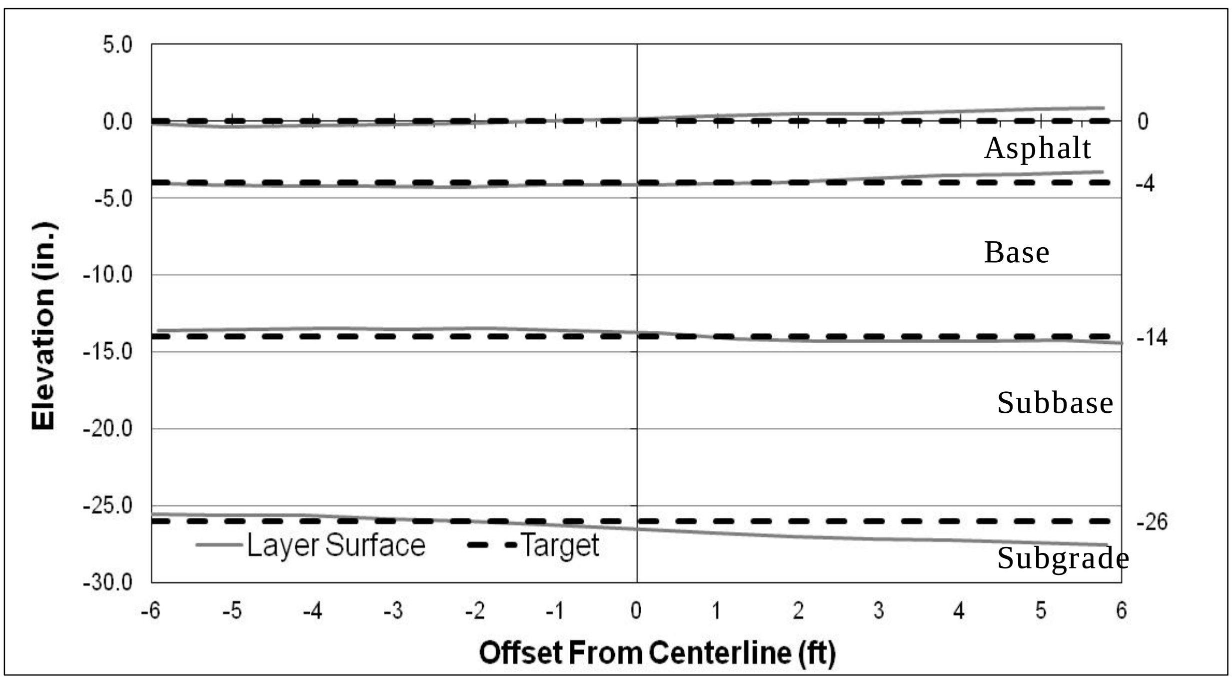

Table 4. Summary of as-constructed layer thicknesses.

| | Subgrade (in.) | | Subbase (in.) | | Base (in.) | | Asphalt (in.) | |
|---|---|---|---|---|---|---|---|---|
| Item | Avg. | Std. Dev. | Avg. | Std. Dev. | Avg. | Std. Dev. | Avg. | Std. Dev. |
| HMA | 22 | --- | 12.4 | 0.4 | 9.4 | 0.3 | 4.2 | 0.1 |
| Foam | 22 | --- | 12.2 | 0.4 | 9.7 | 0.4 | 4.1 | 0.2 |
| Sasobit® | 22 | --- | 12.1 | 0.3 | 9.5 | 0.3 | 4.2 | 0.2 |
| Evotherm™ | 22 | --- | 12.3 | 0.5 | 10.2 | 0.5 | 4.2 | 0.1 |

Note: Thickness values are for the central 40 ft x 8 ft area of each item where traffic was applied.

## Instrumentation

Figure 54 shows the instrumentation layout used in this study. Each test item was instrumented with surface strain gauges, I-buttons, ASGs, SDDs, and EPCs to measure the pavement response to simulated aircraft loading. The asphalt concrete strain gauges (Figure 55) were installed on top of the limestone base to measure deformations at the bottom of the asphalt layer. These gauges were installed by screening HMA over a #4 sieve and using the fine portion to create a thin, compacted dome over the gauge to protect it during paving (Figure 56). Surface strain gauges were installed at the asphalt surface. The EPC's (Figures 57 and 58) and SDD's (Figure 59) were installed in the subgrade, subbase and base layers to evaluate the response of the sub-layers underneath the asphalt surface. I-buttons were installed in the asphalt layer to continuously measure temperature near the surface, middepth and at the bottom of the asphalt layer. During traffic testing, two I-buttons were also placed above the pavement surface to measure air temperature. A moisture sensor (Figure 60) was installed in the subgrade to ensure the subgrade did not change strength over time.

Figure 54. Typical instrumentation layout for each item.

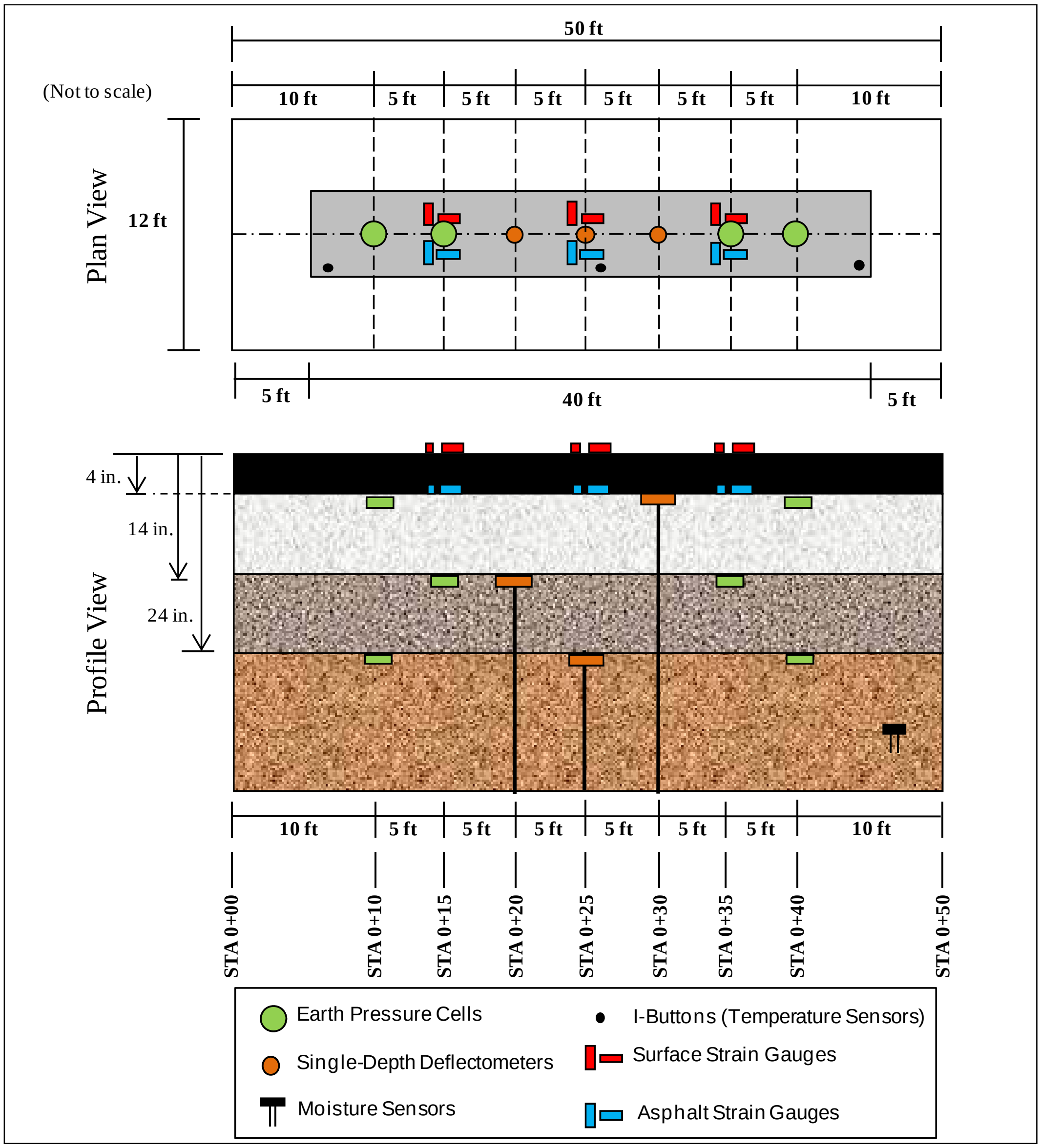


Figure 55. Asphalt strain gauge.

Figure 56. Installing asphalt strain gauge.

Figure 57. Earth pressure cell.

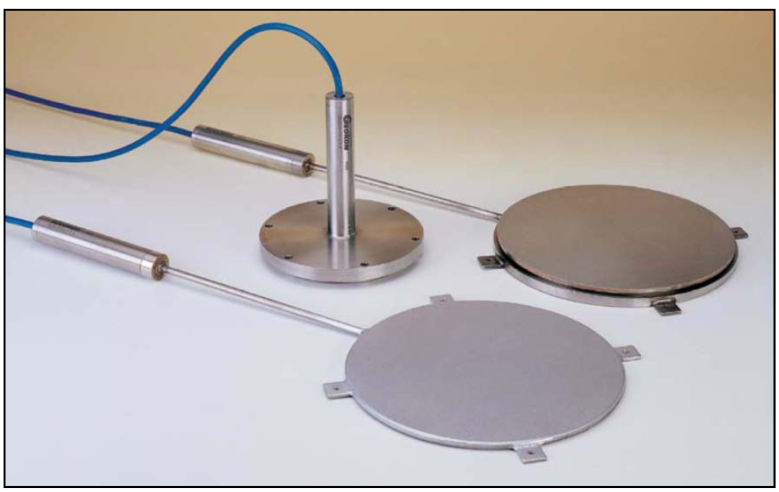

Figure 58. Typical earth pressure cell installation.

Figure 59. Typical SDD gauge installation.

Figure 60. Soil moisture sensor.

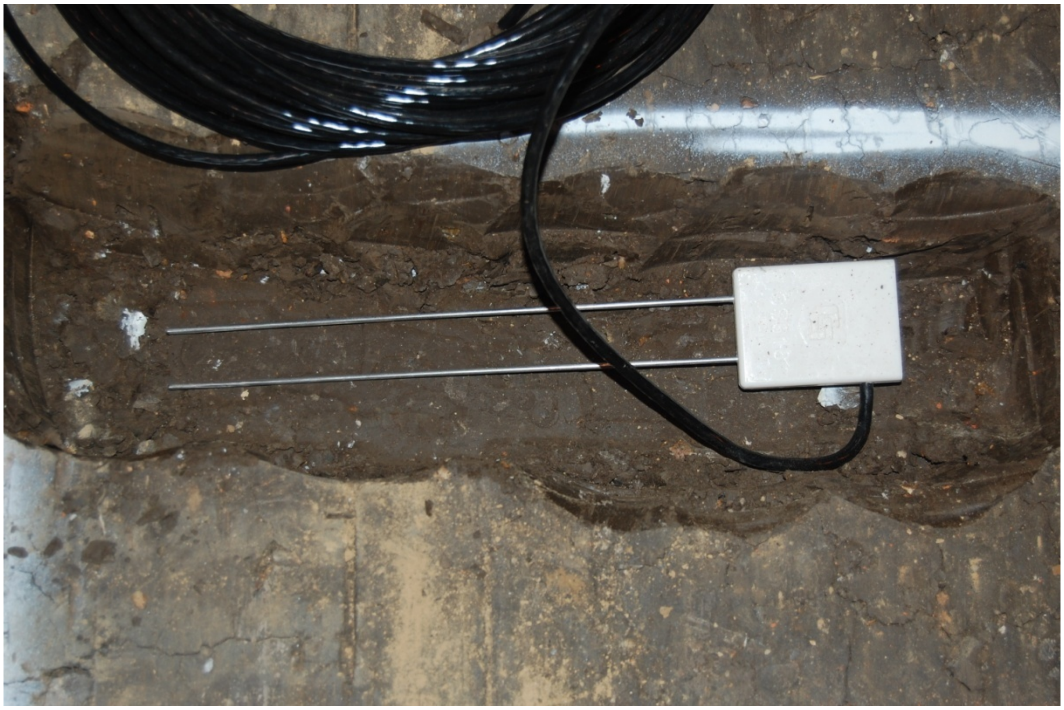

# 4 WMA Mix Production and Placement Procedures Compared to HMA

Data were collected during production and placement of the WMA and HMA to determine if lowering the production temperature affects construction procedures. The following paragraphs detail the data collected during production at the asphalt plant, transportation to the placement site, and during placement and compaction.

## Plant operations

Aggregate handling procedures at the asphalt plant were no different for WMA or HMA. The same aggregate blend was used for each mixture. Samples were taken from the stockpiles and from the feed belt before and during production to measure stockpile moisture content. The results are given in Table 5. Rain on days preceding production increased the stockpile moisture content to nearly 6 percent. On production days, the moisture content was approximately 5 and 4 percent. Samples from the feed belt indicated an average moisture content of 4 to 5 percent.

Table 5. Combined aggregate moisture contents at asphalt plant.

| Moisture Content | | | |
|---|---|---|---|
| From Stockpiles | | | |
| 6/8/2012 | 6/13/2012 | 6/14/2012 | 6/15/2012 |
| 3.0% | 5.8% | 4.9% | 4.0% |
| From Belt Feed | | | |
| 6/14/2012 AM | 6/14/2012 PM | 6/15/2012 AM | 6/15/2012 PM |
| 4.2% | 4.4% | 4.2% | 5.2%[a] |

[a] different sand stockpile used with higher moisture content

Aggregate was recovered from mixture sampled at the plant using trichloroethylene solvent extraction according to AASHTO T 164 Method A. The results from the gradation of the extracted aggregate according to AASHTO T 30 are shown in Figure 61 along with the JMF blend. The plant-produced blend had slightly higher dust content but was very near the design gradation. Some production of dust is expected due to aggregate breakdown. Results were not affected by the WMA technology used.

Figure 61. Plant-produced and JMF aggregate blend.

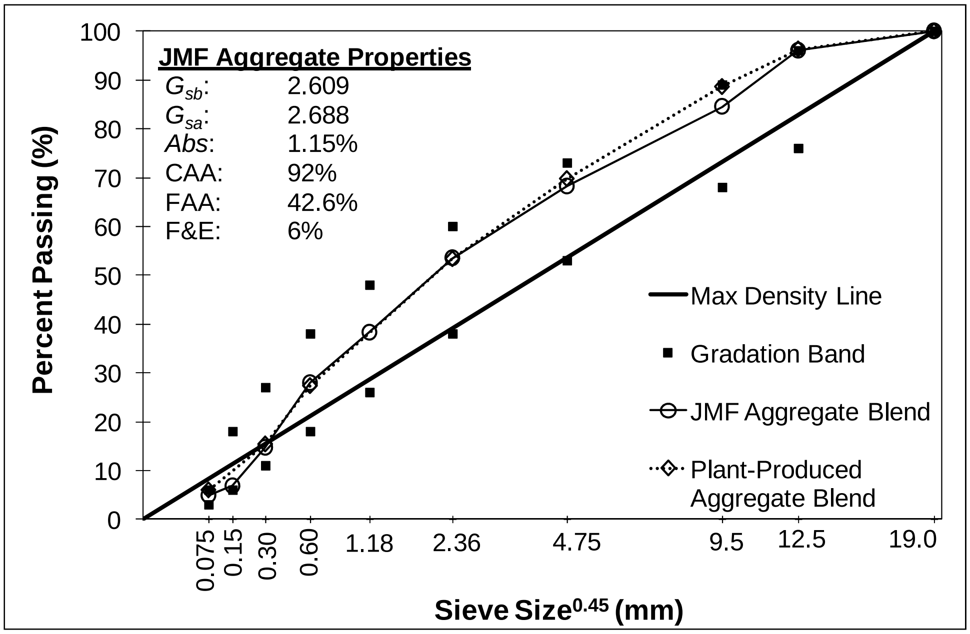


The moisture content of the asphalt mixture was measured according to AASHTO T 329. Results are given in Table 6. Some in the industry have questioned if WMA is more likely to have retained moisture in the mixture since the production temperature is lower and less heat is available to evaporate moisture. As noted in Table 5, the moisture content of the stockpiles was somewhat high due to rain before the production dates. The first lift of HMA had the lowest moisture content of 0.06 percent. The lower moisture content may have been caused by higher production temperatures. However, the moisture content of the second lift of HMA was 0.12 percent. This value was similar to most of the WMA samples. The highest moisture content was the second lift of the foamed asphalt, 0.16 percent. The moisture content may have been raised by the addition of water during the foaming process. All of the moisture contents were below the maximum of 0.5 percent, allowed in UFGS 32 12 15.13.

Specimens of asphalt mixture were compacted in two different laboratories to determine volumetric properties. The contractor's laboratory at the asphalt plant was used for quality control (QC) tests. ERDC's laboratory near the laydown site was used for quality assurance (QA) tests. Table 7 provides pertinent mixture properties for each item as measured by both laboratories. The average result from two specimens is reported.

Table 6. Moisture content of asphalt mixtures.

| Test Item | Lift | AC Mix Moisture Content (%) |
|---|---|---|
| HMA | 1st | 0.06 |
| | 2nd | 0.12 |
| Sasobit® | 1st | 0.11 |
| | 2nd | 0.12 |
| Foamed Asphalt | 1st | 0.10 |
| | 2nd | 0.16 |
| Evotherm™ | 1st | 0.12 |
| | 2nd | 0.14 |

Table 7. Laboratory volumetric mixture properties.

| Mix ID | $G_{mm}$ | $G_{se}$ | $G_{mb}$ | $P_b$ | $P_{ba}$ | $P_{be}$ | $V_a$ | VMA | VFA | D/B |
|---|---|---|---|---|---|---|---|---|---|---|
| **Target** | — | — | — | — | — | — | 4 | min 14.0 | 65-78 | 0.8-1.2 |
| HMA-QC[a] | 2.444 | 2.645 | 2.388 | 5.3 | 0.54 | 4.75 | 2.3 | 13.3 | 83 | 1.20 |
| Sasobit®-QC[a] | 2.442 | 2.643 | 2.389 | 5.3 | 0.51 | 4.77 | 2.2 | 13.3 | 84 | 1.09 |
| Evotherm™-QC[a] | 2.456 | 2.650 | 2.413 | 5.0 | 0.61 | 4.46 | 1.7 | 12.2 | 86 | 1.29 |
| Foam-QC[a] | 2.448 | 2.638 | 2.402 | 5.0 | 0.43 | 4.55 | 1.9 | 12.5 | 85 | 1.24 |
| HMA-QA[b] | 2.454 | 2.659 | 2.399 | 5.3 | 0.74 | 4.58 | 2.3 | 12.9 | 82 | 1.16 |
| Sasobit®-QA[b] | 2.460 | 2.650 | 2.384 | 4.9 | 0.61 | 4.33 | 3.1 | 13.1 | 76 | 1.21 |
| Evotherm™-QA[b] | 2.463 | 2.652 | 2.414 | 4.9 | 0.64 | 4.27 | 2.0 | 12.0 | 83 | 1.61 |
| Foam-QA[b] | 2.471 | 2.660 | 2.356 | 4.8 | 0.76 | 4.11 | 4.7 | 14.1 | 67 | 1.50 |

Note: An asphalt binder $G_b$ = 1.03 was used for all calculations.

a) Average results from producer's Quality Control (QC) testing.

b) Average results from researcher's Quality Assurance (QA) testing.

The maximum theoretical specific gravity, $G_{mm}$, determined from QC testing was slightly lower than that determined during QA testing. This slight difference did not appear to have a significant impact on other volumetric properties. In general, the QC and QA test results were similar to each other and within the typical level of variation to be expected during construction. The laboratory air voids were lower than the JMF design. Some additional dust in the mixture may have reduced the air voids. This explanation is supported by the reduced VMA and increased VFA for the mixtures. These deviations from the JMF are common during asphalt concrete production. The main difference in test results for these materials is the higher air void content of the foamed asphalt during QA testing compared to QC test results. This mixture had the lowest temperature

when it arrived at the lay down site. The lower temperature during QA testing may have caused the $G_{mb}$ to be low; therefore, increasing air voids and VMA. In general, the WMA did not cause any difference in measured volumetric properties compared to the HMA.

Details of the transportation process were recorded to determine if the time between mixing at the asphalt plant and paving influenced mixture or pavement properties. The haul times reported in this study (Table 8) are not expected to have a significant impact on mixture performance. Once the mixture left the drum and was placed into the storage silo, it was transferred to the transport trucks for delivery to the laydown site. For most lifts, the mixture was delivered in two truckloads. Only one truckload was delivered for the first lift of Evotherm™. This truck contained sufficient mixture to pave the full lane. According to these data, the average haul time was just below 20 minutes. The total time between production of mixture at the asphalt plant and dumping the mixture into the paver was an average of just under an hour; though the time ranged from about 30 minutes to around 2 hours. The longest period of time was for the second lift of the HMA item that was produced in the morning but did not leave the plant until after a break in work for lunch. The total time from mixing to placement and compaction was generally less than the two-hour laboratory conditioning used for mix design period described in Doyle et al. (in preparation).

The QA data indicate that slightly less binder absorption took place during plant production compared to the laboratory mix design; while the QC tests indicate less absorption than the QA tests. This is reasonable, since the QC tests were performed approximately 30 minutes prior to the QA tests, allowing the mixture additional time to absorb binder. It is important to note that realistic storage times are needed for accurate volumetric property measurements during mixture design.

## Placement and compaction

The asphalt mixtures were monitored during placement and compaction to determine if WMA required any different construction considerations from HMA. Data collected during these processes included temperature of the mixture during paving and compaction, density of the asphalt layer during compaction, and the number and type of roller passes required to achieve adequate mat density.

Table 8. Transport truck data.

| Date | Truck ID | Mix Description | Time Mix Produced | Time Left Plant | Time Arrived Hangar 4 | Time Poured Mix to Paver | Hauling Time, hr: min | Waiting Time, hr: min | Total Time, hr: min |
|---|---|---|---|---|---|---|---|---|---|
| 6/14/2012 | 113 | HMA | 8:29 | 8:46 | 9:05 | 9:18 | 0:19 | 00:30 | 00:49 |
| 6/14/2012 | 118 | HMA | 8:35 | 8:49 | 9:06 | 9:22 | 0:17 | 00:30 | 00:47 |
| 6/14/2012 | 113 | Sasobit® | 10:03 | 10:18 | 10:36 | 10:45 | 0:18 | 00:24 | 00:42 |
| 6/14/2012 | 118 | Sasobit® | 10:08 | 10:20 | 10:39 | 10:50 | 0:19 | 00:23 | 00:42 |
| 6/14/2012 | 113 | HMA | 10:52 | 12:29 | 12:48 | 12:56 | 0:19 | 01:45 | 02:04 |
| 6/14/2012 | 118 | HMA | 10:59 | 12:33 | 12:55 | 13:05 | 0:22 | 01:44 | 02:06 |
| 6/14/2012 | 113 | Sasobit® | 13:19 | 13:33 | 13:55 | 13:59 | 0:22 | 00:18 | 00:40 |
| 6/14/2012 | 118 | Sasobit® | 13:26 | 13:35 | 14:02 | 14:10 | 0:27 | 00:17 | 00:44 |
| 6/15/2012 | 113 | Foam | 8:30 | 8:47 | 9:03 | 9:19 | 0:16 | 00:33 | 00:49 |
| 6/15/2012 | 118 | Foam | 8:36 | 8:48 | 9:07 | 9:25 | 0:19 | 00:30 | 00:49 |
| 6/15/2012 | 113 | Evotherm™ | 10:12 | 10:27 | 10:45 | 10:53 | 0:18 | 00:23 | 00:41 |
| 6/15/2012 | 118 | Foam | 12:26 | 12:34 | 12:48 | 12:55 | 0:14 | 00:15 | 00:29 |
| 6/15/2012 | 113 | Foam | 12:30 | 12:36 | 12:50 | 13:03 | 0:14 | 00:19 | 00:33 |
| 6/15/2012 | 118 | Evotherm™ | 13:02 | 13:17 | 13:35 | 13:51 | 0:18 | 00:31 | 00:49 |
| 6/15/2012 | 113 | Evotherm™ | 13:06 | 13:19 | 13:36 | 13:56 | 0:17 | 00:33 | 00:50 |
| Average | | | | | | | 0:18 | 00:35 | 00:54 |

Figures 62 through 65 show infrared images of the mixtures as they emerge from the paver. The scale at the right of the figures provides the range of temperatures in each image. In general, the asphalt layers do not show significant thermal segregation. The maximum temperature of the mixtures does show large differences. As expected, the HMA was placed at the highest temperature. As seen in Figure 62, the temperature of the HMA was approximately 280°F (138°C) during paving. This temperature is appropriate for an unmodified PG 67-22 binder. The temperature of the foamed asphalt mixture during paving was approximately 230°F (110°C). This mixture had the greatest temperature reduction (50°F) of any of the warm mixtures. The Sasobit® and Evotherm™ mixtures were paved at approximately 265°F (130°C). This temperature was above the 240°F compaction temperature used in laboratory mix design.

Figures 66 through 69 show additional temperature measurements along with density measurements taken during compaction. Density (left axis) and surface temperature (right axis) measurements are shown as a function of number of roller passes. The surface temperature measurements are from

Figure 62. Infrared picture of HMA placement.

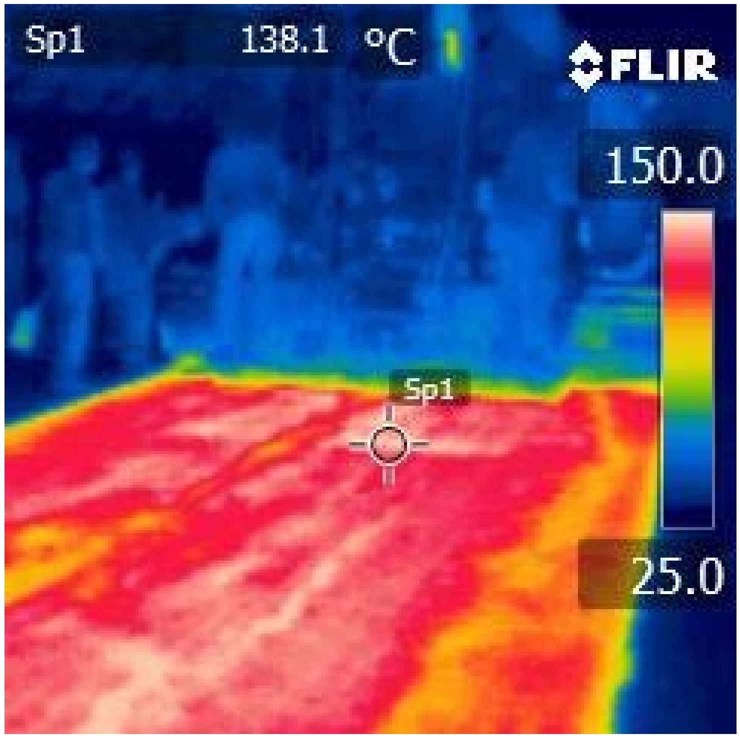


Figure 63. Infrared picture of foamed asphalt placement.

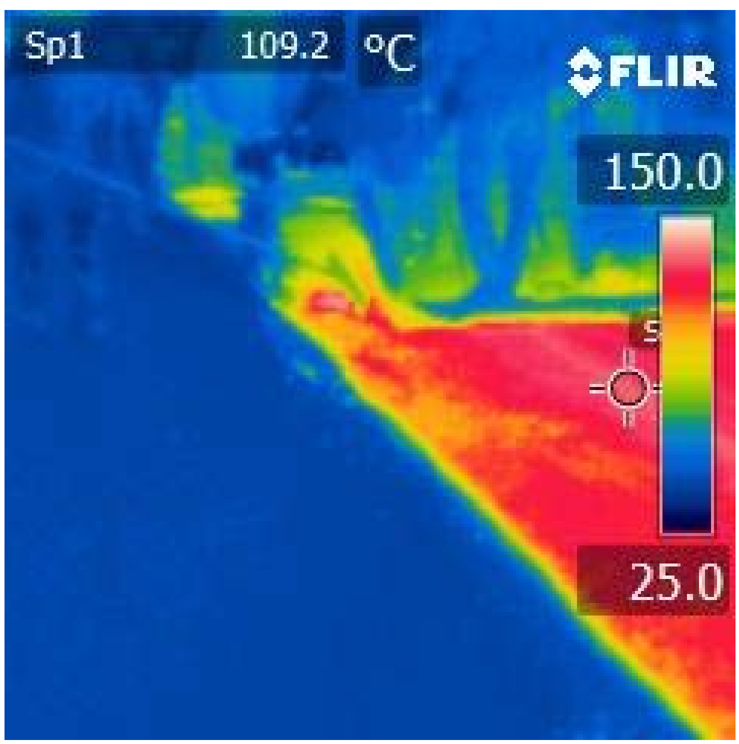

Figure 64. Infrared picture of Sasobit® WMA placement.

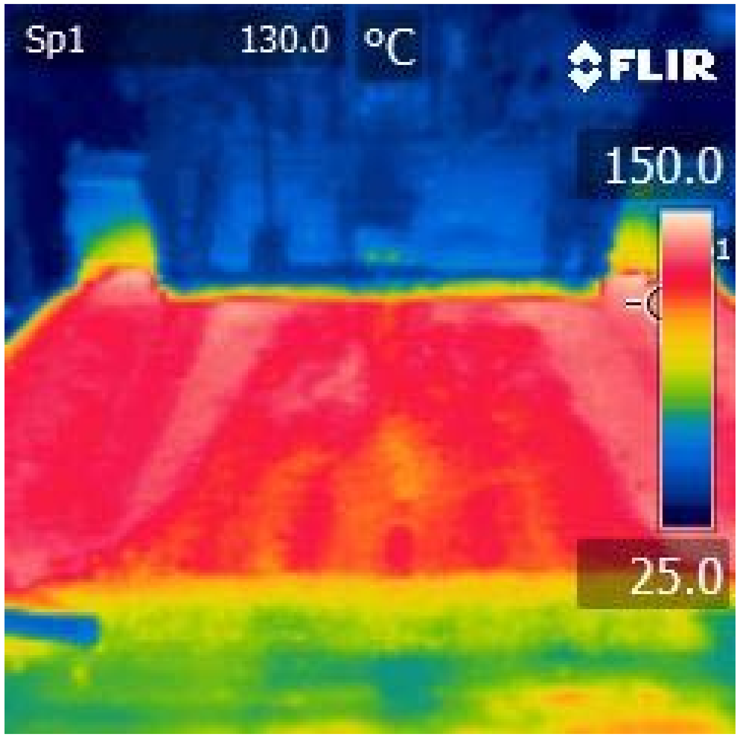


Figure 65. Infrared picture of Evotherm™ WMA placement.

Figure 66. Compaction of HMA.

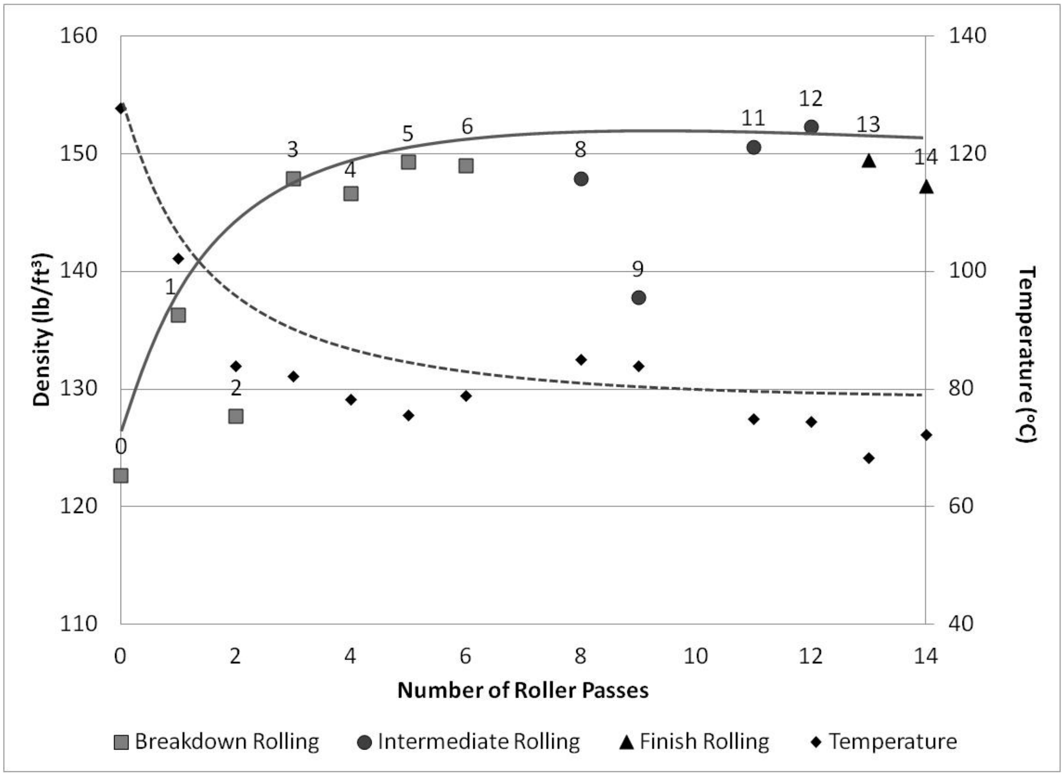


Figure 67. Compaction of foamed asphalt.

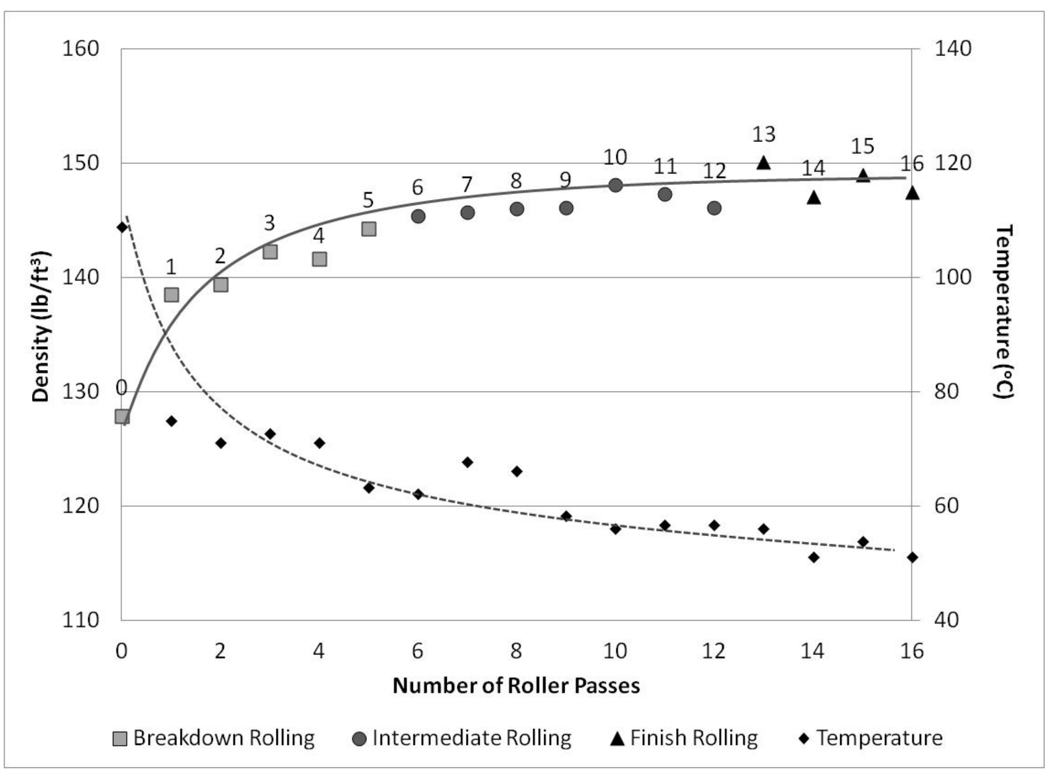

Figure 68. Compaction of Sasobit® WMA.

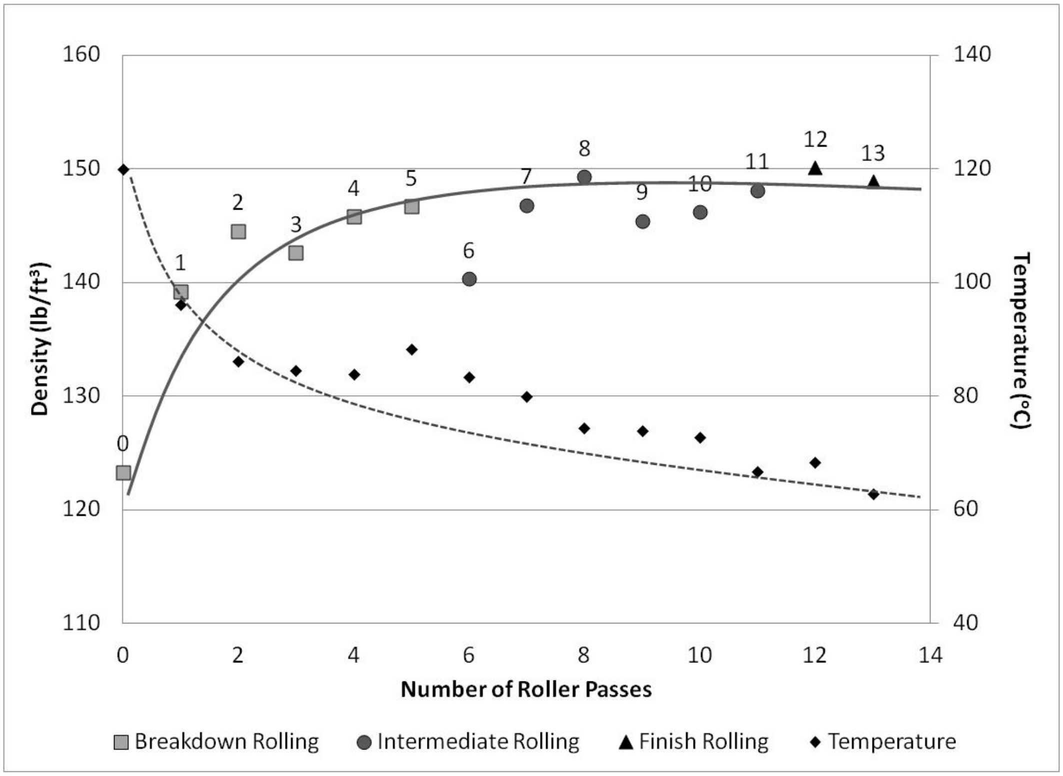


Figure 69. Compaction of Evotherm™ WMA.

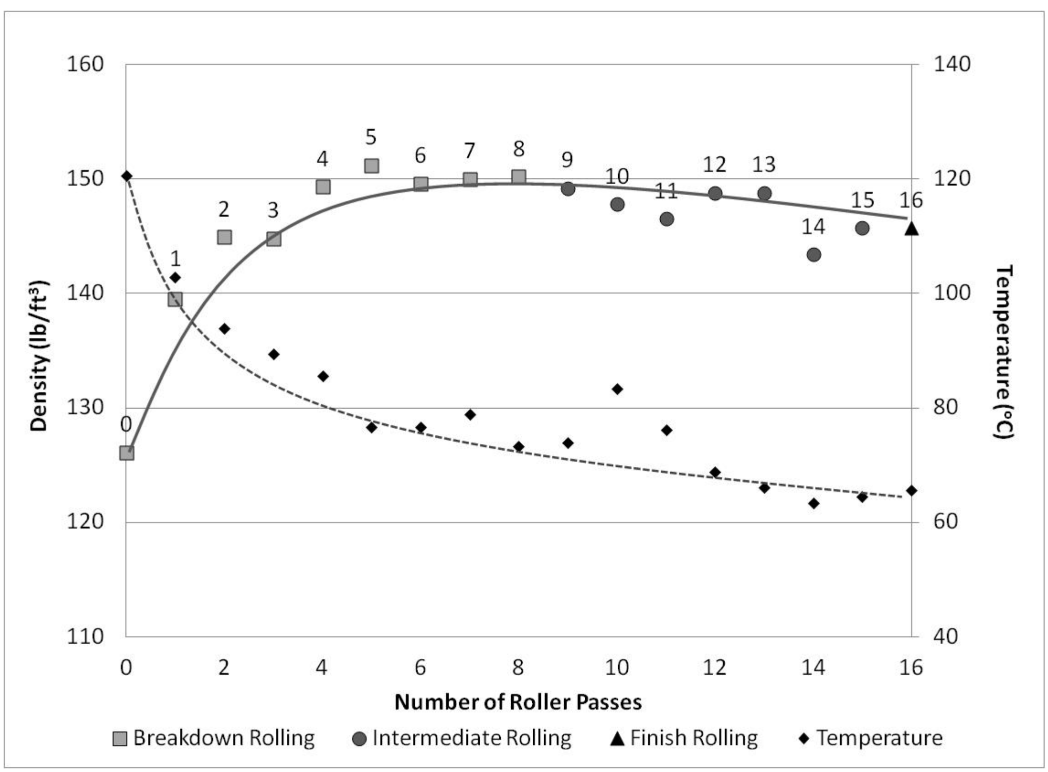

an infrared temperature gun. Average maximum temperature values were recorded throughout compaction. Density measurements were taken with a Troxler nuclear density gauge in backscatter mode. The type of roller used for each pass is indicated on each figure. The contractor determined how many roller passes to use on each item. Final compaction was ceased based upon appearance and density measurements.

The roller pattern was very similar for each of the mixtures. Having a lower temperature did not require additional compaction to achieve the target density. The final density of each item was approximately 150 lb/ft$^3$ after compaction. Most of the compaction was achieved during breakdown rolling with the steel-wheeled vibratory roller. The number of roller passes for breakdown rolling varied between five and eight on the different items. Either six or seven passes of the pneumatic roller were applied to each item. Finally, between one and four passes of the static steel-wheeled roller were used for finish rolling.

The foamed asphalt section had a slightly lower rate of compaction than the other sections. For example, the density of this item did not reach 145 lb/ft$^3$ until after 5 passes with the breakdown roller. This same density was achieved with only two or three passes on other sections. However, the temperature was lower on the foamed asphalt item. The surface temperature started at 110$^o$C and had cooled to 60$^o$C after 8 roller passes. The temperature never cooled below 60$^o$C on any other item during compaction. The higher stiffness resulting from the cooler mix may have resulted in the lower rate of densification. Temperature measurements from the infrared gun device were very similar to measurements from the thermal camera. The HMA had the highest initial surface temperature of 130$^o$C. The Sasobit® and Evotherm™ each had initial measured surface temperatures of 120$^o$C.

A final measurement of the asphalt concrete temperature was made using thermocouples embedded at the approximate middepth of each lift (1 in. deep). The thermocouples were installed by attaching them to a small metal rod and inserting the rod immediately after the paver laid the mixture. The rod was inserted approximately 1 ft. into the mixture. Figures 70 through 73 show the temperature at this location for each mix. These figures include measurements for both the first and second lift that were paved. These thermocouples remained in place throughout construction. In each case, the temperature of the first lift had cooled to approximately 10$^o$C above air

temperature by the time the second lift was placed. Once the second lift was placed, the temperature of the first lift begins to increase. The lift temperatures begin to equalize as the surface cools. These thermocouple measurements confirm the mixture temperatures reported by the other two measurement methods. The HMA paving temperature was between 130°C and 140°C. The foamed asphalt was paved near 110°C. The Sasobit® thermocouple did not capture the initial pavement temperature. The Evotherm™ was paved at approximately 120°C.

Figure 70. Temperature of HMA pavement during construction.

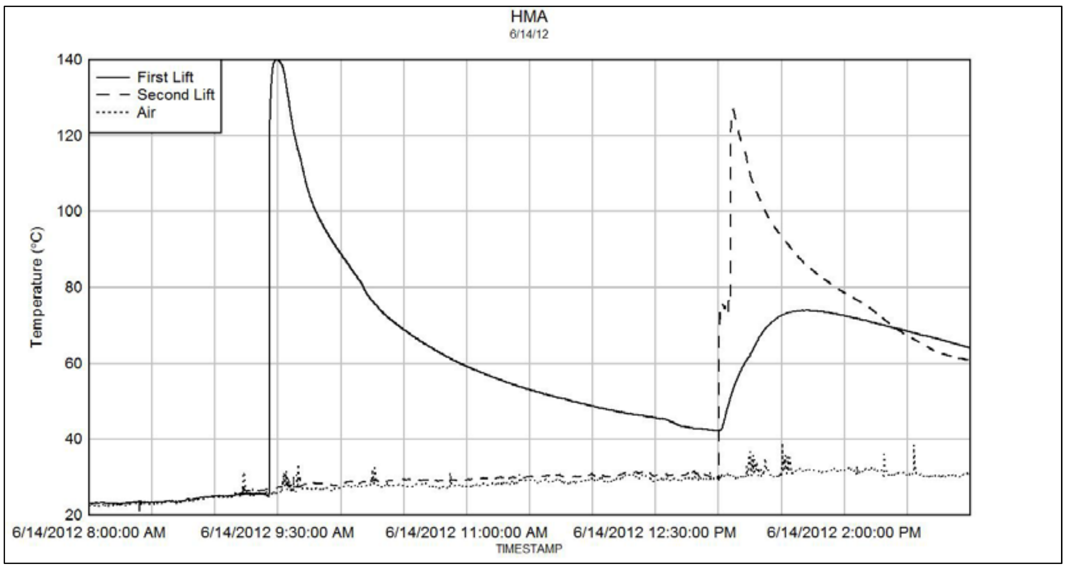


Figure 71. Temperature of foamed asphalt pavement during construction.

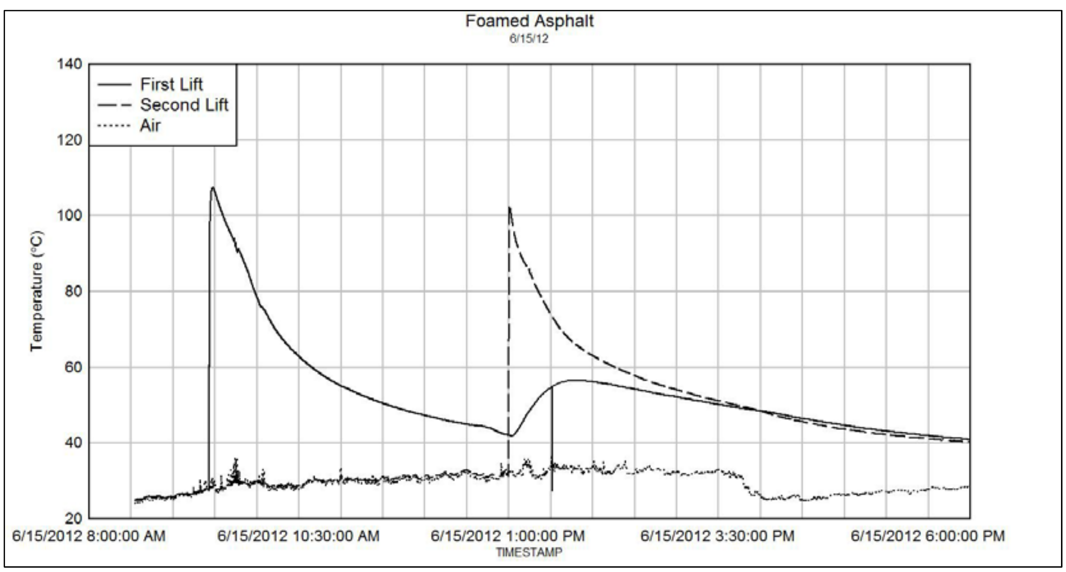

Figure 72. Temperature of Sasobit® WMA pavement during construction.

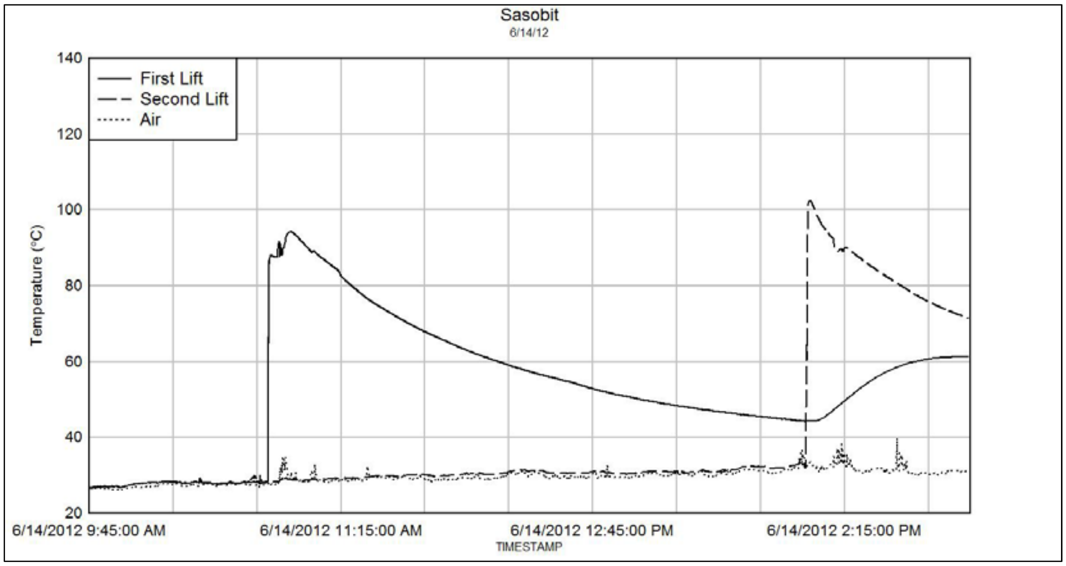


Figure 73. Temperature of Evotherm™ WMA pavement during construction.

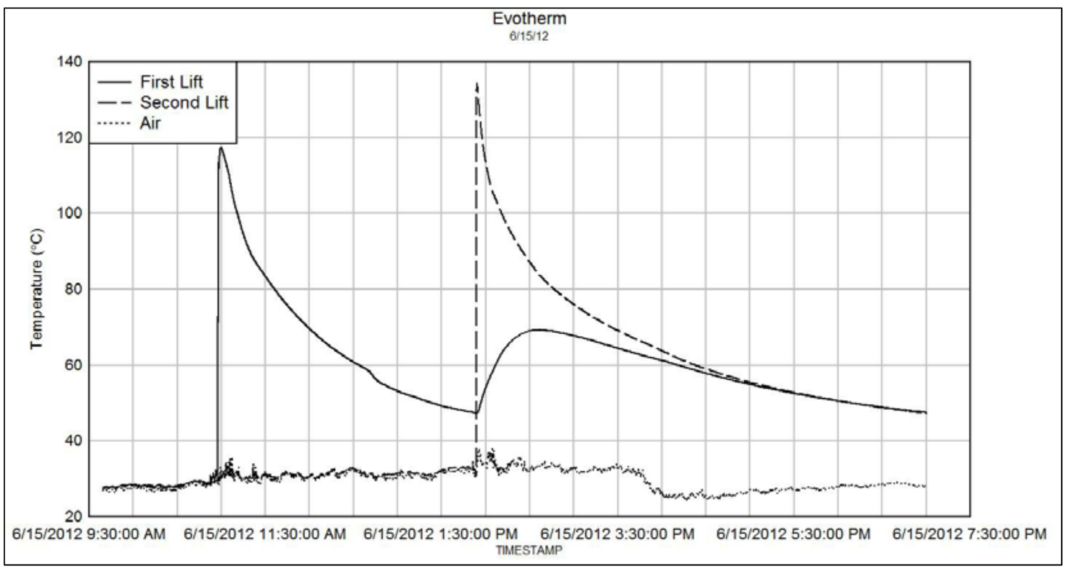


## Measurements on asphalt cores

Cores were extracted from the asphalt concrete pavement sections to determine the in-situ volumetric properties. The coring pattern for each item is shown in Figure 74. Table 9 provides average values for 12 cores taken from each item. The $G_{mm}$ and percent binder, $P_b$, values were determined from QA lab testing. The $G_{mb}$ was measured according to AASHTO T166.

Figure 74. Layout for post construction coring of each test item.

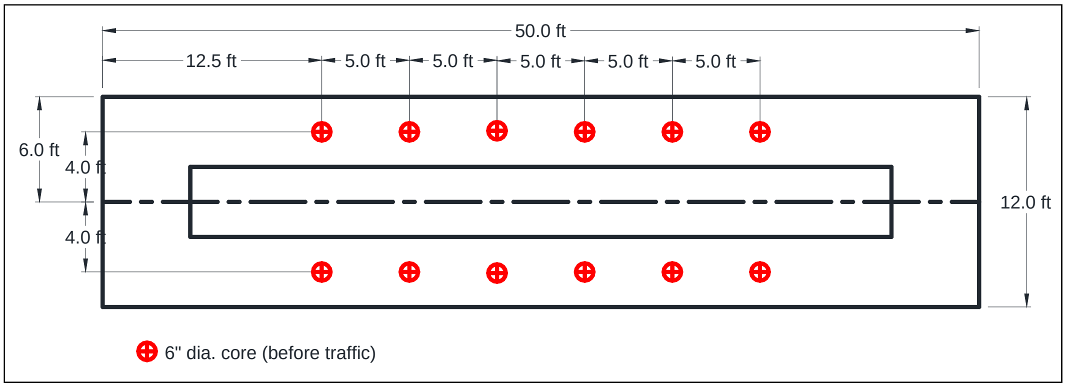


Table 9. Volumetric properties of asphalt cores.

| Mix ID | $G_{mm}$ | $G_{mb}$ | $P_b$ | $V_a$ | VMA | VFA | Thickness |
|---|---|---|---|---|---|---|---|
| **Target** | — | — | — | 4.0-6.0 | ≥ 14.0 | 65-78 | 4.0 |
| HMA | 2.454 | 2.360 | 5.3 | 3.8 | 14.3 | 73 | 4.2 ± 0.16 |
| Foamed Asphalt | 2.471 | 2.322 | 4.8 | 6.0 | 15.3 | 61 | 4.1 ± 0.31 |
| Sasobit® | 2.460 | 2.351 | 4.9 | 4.4 | 14.3 | 69 | 4.2 ± 0.23 |
| Evotherm™ | 2.463 | 2.345 | 4.9 | 4.8 | 14.5 | 67 | 4.2 ± 0.26 |

The compacted air voids was close to the lower end of the target air void range for the HMA, Sasobit®, and Evotherm™. The foamed asphalt item had the highest air void content at the upper end of the target range. This item was also compacted at the lowest temperature and was approximately 10°C cooler than the other WMAs during compaction. During construction, it did not achieve density as quickly as the other items. Its final density was lower than the other items, resulting in higher air voids. The higher VMA and lower VFA values resulted from lower density. Overall, the total thickness of the items was close to the target value of 4.0 inches.

# 5 Discussion

The objective of the work described in this report was to compare production and construction procedures of WMA and HMA. Plant operations, equipment requirements, transportation procedures, and placement and compaction procedures were studied to determine if WMA has unique requirements for construction compared to HMA.

The contractor was able to provide the HMA and WMA using the same production equipment. Procedures for producing each mixture were the same in terms of plant operations. The only unique requirement for WMA was supplying the additive. The Evotherm™ was pre-blended with the binder at the asphalt supplier's terminal and did not require any special equipment. The Sasobit® and foamed asphalt required an external feed source to inject the additive or water into the mixing drum. The WMA industry reports that the cost of additional equipment is easily recovered by reduced fuel consumption from lower production temperatures.

The procedures for placing and compacting the WMA were the same as for the HMA. Although the mixture was delivered at lower temperature, the rolling pattern was very similar for HMA and WMA. The WMA additives appeared to provide additional workability at lower temperatures to allow for sufficient compaction of the mixtures.

Data collected during compaction showed that the foamed asphalt section was compacted at a lower temperature than the other two WMAs. The temperature of this item was approximately 50°F (28°C) cooler than the HMA. This large reduction in temperature made the foamed asphalt mixture somewhat more difficult to compact according to density measurements obtained in this study; however, adequate densities were achieved with a similar amount of compaction effort. The two other WMAs compacted approximately 20°F (11°C) cooler than the HMA and showed similar ability to compact.

The procedures for evaluating material properties during QC or QA were not impacted by the use of WMA. Volumetric properties should be determined the same way as traditionally measured for HMA. The design percent air voids and VMA could be achieved with WMA produced at full scale. The

addition of moisture or the production of the mixture at lower temperature did not cause excessive moisture to remain in the mixture. In fact, moisture tests on the mixtures indicated they had only about 25 percent of the allowable maximum moisture according to UFGS 32 12 15.13.

# 6 Conclusions and Recommendations

## Conclusions

The following conclusions resulted from evaluating WMA produced at full scale compared to a similar mixture produced as HMA:

- WMA can be produced, placed, and compacted at temperatures at least 20°F (11°C) lower than a HMA using the same aggregate, while achieving equivalent density using traditional 2-in. lift thickness. The ability to achieve equivalent density was successfully demonstrated using Sasobit® and Evotherm™ admixtures.
- The pavement section constructed using foamed asphalt had lower in-place density than the HMA or other WMA items. The temperature of the foamed asphalt was nearly 50°F (28°C) cooler than the HMA. As with all asphalt paving mixtures, reducing temperature makes compaction more difficult. The foamed asphalt pavement met density requirements for 100 percent pay according to UFGS 32 12 15.13.
- The aggregates used in production had relatively high moisture content because of rain preceding construction. Even so, producing mixtures at WMA temperatures did not cause excessive moisture to be retained in the mixture.
- UFGS 32 12 15.16, WMA for Airfields, should be sufficient to govern constructing airfield pavements with a WMA surface.

## Recommendations

As a result of evaluating the full-scale production and placement of WMA, it is recommended that performance testing be continued on the test items as planned using simulated traffic. No critical findings from this portion of the study would preclude the use of WMA for airfield pavements. Few modifications to construction specifications would be required to allow contractors to place WMA in lieu of HMA. These modifications would mostly be limited to terminology and temperature ranges. The simulated traffic testing should provide an indication of WMA rutting performance compared to HMA. Long-term performance of WMA compared to HMA should be documented once trials of WMA are placed on active military airfield installations.

# References

American Association of State Highway and Transportation Officials. 2012. *Bulk specific gravity ($G_{mb}$) of compacted Hot Mix Asphalt (HMA) using saturated surface-dry specimens*. Washington DC: AASHTO Designation T 166.

American Association of State Highway and Transportation Officials. 2012. *Theoretical maximum specific gravity ($G_{mm}$) and density of Hot Mix Asphalt (HMA).* Washington DC: AASHTO Designation T 209.

American Association of State Highway and Transportation Officials. 2010. *Bulk specific gravity ($G_{mb}$) and density of compacted Hot Mix Asphalt (HMA) using vacuum sealing method.* Washington DC: AASHTO Designation T 331.

American Association of State Highway and Transportation Officials. 2008. *Moisture content of Hot Mix Asphalt (HMA) by oven method.* Washington DC: AASHTO Designation T 329.

American Society for Testing and Materials International (ASTM). 2007. *Standard test method for CBR (California Bearing Ratio) of laboratory-compacted soils*. Designation: D 1883-07e2. West Conshohocken, PA.

ASTM International. 2007. *Standard test method for density and unit weight of soil in place by the sand-cone method.* Designation: D 1556-07. West Conshohocken, PA: American Society for Testing and Material.

ASTM International. 2008. *Standard test method for determination of water (moisture) content of soil by microwave oven heating*. Designation: D 4643-08. West Conshohocken, PA: American Society for Testing and Material.

ASTM International. 2009. *Standard test method for CBR (California Bearing Ratio) of soils in place*. Designation: D 4429-09a. West Conshohocken, PA: American Society for Testing and Material.

ASTM International. 2010. *Standard test method for in-place density and water content of soil and soil-aggregate by nuclear methods (shallow depth)*. Designation: D 6938-10. West Conshohocken, PA: American Society for Testing and Material.

ASTM International. 2010. *Standard test method for density of soil in place by the drive-cylinder method*. Designation: D 2937-10. West Conshohocken, PA: American Society for Testing and Material.

ASTM International. 2011. *Standard practice for classification of soils for engineering purposes* (Unified Soil Classification System). Designation: D 2487-11. West Conshohocken, PA: American Society for Testing and Material.

ASTM International. 2012. *Standard test methods for laboratory compaction characteristics of soil using modified effort* (56,000 ft-lbf/ft$^3$ (2,700 kN-m/m$^3$)). Designation: D 1557-12. West Conshohocken, PA: American Society for Testing and Material.

Department of the Air Force, Headquarters Air Force Civil Engineer Support Agency. 2011. Engineering Technical Letter (ETL) 11-3. *Warm Mix Asphalt (WMA)*, Tyndall AFB, FL: US Department of Defense.

Doyle, J. D., J. F. Rushing, and M. Mejías-Santiago (in preparation). *Laboratory performance testing of warm-mix asphalt (wma) technologies for airfield pavements*. ERDC/GSL-TR-13-XX. Vicksburg, MS: US Army Engineer Research and Development Center, Geotechnical and Structures Laboratory.

Headquarters, Departments of the Army, the Navy, and the Air Force. 2001b. *Pavement design for airfields*. Washington, DC: Unified Facilities Criteria (UFC) 3-260-02.

Headquarters, Departments of the Army, the Navy, and the Air Force. 2012. Unified Facilities Guide Specification 32 12 15.13. *Hot Mix Asphalt (HMA) for airfields*. Washington, DC: US Department of Defense.

Headquarters, Departments of the Army, the Navy, and the Air Force. 2012. Unified Facilities Guide Specification 32 12 15.16. *Warm mix asphalt (WMA) for airfields*. Washington, DC: US Department of Defense.

Mejías-Santiago, M., J. D. Doyle, I. L. Howard, and E. R. Brown. 2012. *Evaluation of warm-mix asphalt technologies for use on airfield pavements*. ERDC/GSL-TR-12-3. Vicksburg, MS: US Army Engineer Research and Development Center, Geotechnical and Structures Laboratory.

National Cooperative Highway Research Program. 2004. *Laboratory determination of resilient modulus for flexible pavement design*. Research Results Digest Number 285, Washington DC: Transportation Research Board.

The Asphalt Institute. 2007. *The Asphalt Handbook*. Manual Series No. 4 (MS-4), 7th Edition, Lexington, KY: The Asphalt Institute.

Uzan, J. 1985. *Characterization of granular material*. Transportation Research Record. 1022: 52-59.

# Appendix A: Resilient Modulus Data

Table A1. Resilient modulus data for base layer replicate 1.

| Test Sequence | $\sigma_1$ | $\sigma_2$ | $\sigma_3$ | $\theta$ | $\tau$ | $\sigma_1 - \sigma_3$ | $M_R$ | Pred. $M_R$ |
|---|---|---|---|---|---|---|---|---|
| | psi | psi | psi | psi | psi | psi | psi | psi |
| 1 | 6.5 | 3.1 | 3.1 | 12.7 | 1.6 | 3.4 | 20,161 | 17,234 |
| 2 | 11.6 | 6.1 | 6.1 | 23.8 | 2.6 | 5.5 | 29,513 | 29,438 |
| 3 | 18.4 | 10.1 | 10.1 | 38.6 | 3.9 | 8.3 | 41,619 | 43,738 |
| 4 | 26.9 | 15.1 | 15.1 | 57.1 | 5.6 | 11.8 | 58,146 | 59,390 |
| 5 | 35.6 | 20.1 | 20.1 | 75.8 | 7.3 | 15.5 | 75,746 | 73,204 |
| 6 | 8.0 | 3.1 | 3.1 | 14.2 | 2.3 | 4.9 | 20,355 | 18,607 |
| 7 | 14.6 | 6.1 | 6.1 | 26.8 | 4.0 | 8.5 | 29,970 | 31,327 |
| 8 | 23.4 | 10.1 | 10.1 | 43.6 | 6.3 | 13.3 | 43,379 | 45,591 |
| 9 | 34.4 | 15.1 | 15.1 | 64.6 | 9.1 | 19.3 | 61,353 | 60,523 |
| 10 | 45.3 | 20.1 | 20.1 | 85.5 | 11.9 | 25.2 | 77,909 | 73,206 |
| 11 | 11.0 | 3.1 | 3.1 | 17.2 | 3.7 | 7.9 | 21,640 | 21,140 |
| 12 | 20.5 | 6.1 | 6.1 | 32.7 | 6.8 | 14.4 | 33,106 | 34,630 |
| 13 | 33.3 | 10.1 | 10.1 | 53.5 | 10.9 | 23.2 | 48,877 | 48,865 |
| 14 | 49.3 | 15.1 | 15.1 | 79.5 | 16.1 | 34.2 | 67,119 | 62,908 |
| 15 | 65.5 | 20.1 | 20.1 | 105.7 | 21.4 | 45.4 | 78,345 | 74,330 |
| 16 | 14.0 | 3.1 | 3.1 | 20.2 | 5.1 | 10.9 | 22,574 | 23,434 |
| 17 | 26.5 | 6.1 | 6.1 | 38.7 | 9.6 | 20.4 | 34,938 | 37,562 |
| 18 | 43.2 | 10.1 | 10.1 | 63.4 | 15.6 | 33.1 | 50,766 | 51,743 |
| 19 | 64.4 | 15.1 | 15.1 | 94.6 | 23.2 | 49.3 | 67,725 | 65,313 |
| 20 | 86.0 | 20.1 | 20.1 | 126.2 | 31.1 | 65.9 | 78,079 | 76,104 |
| 21 | 20.0 | 3.1 | 3.1 | 26.2 | 8.0 | 16.9 | 24,364 | 27,465 |
| 22 | 38.5 | 6.1 | 6.1 | 50.7 | 15.3 | 32.4 | 38,332 | 42,518 |
| 23 | 61.2 | 10.1 | 10.1 | 81.4 | 24.1 | 51.1 | 54,650 | 56,269 |
| 24 | 95.0 | 15.1 | 15.1 | 125.2 | 37.7 | 79.9 | 70,557 | 69,895 |
| 25 | 130.6 | 20.1 | 20.1 | 170.8 | 52.1 | 110.5 | 82,654 | 80,472 |
| 26 | 25.3 | 3.1 | 3.1 | 31.5 | 10.5 | 22.2 | 24,258 | 30,554 |
| 27 | 50.5 | 6.1 | 6.1 | 62.7 | 20.9 | 44.4 | 39,339 | 46,646 |
| 28 | 85.9 | 10.1 | 10.1 | 106.1 | 35.7 | 75.8 | 57,566 | 61,476 |
| 29 | 131.8 | 15.1 | 15.1 | 162.0 | 55.0 | 116.7 | 74,180 | 74,827 |
| 30 | 174.4 | 20.1 | 20.1 | 214.6 | 72.7 | 154.3 | 90,070 | 84,702 |

Table A2. Resilient modulus data for base layer replicate 2.

| Test Sequence | $\sigma_1$ | $\sigma_2$ | $\sigma_3$ | $\theta$ | $\tau$ | $\sigma_1 - \sigma_3$ | $M_R$ | Pred. $M_R$ |
|---|---|---|---|---|---|---|---|---|
| | psi | psi | psi | psi | psi | psi | psi | Psi |
| 1 | 6.5 | 3.1 | 3.1 | 12.7 | 1.6 | 3.4 | 18,334 | 16,049 |
| 2 | 11.6 | 6.1 | 6.1 | 23.8 | 2.6 | 5.5 | 28,841 | 28,850 |
| 3 | 18.3 | 10.1 | 10.1 | 38.5 | 3.9 | 8.2 | 42,337 | 44,153 |
| 4 | 26.9 | 15.1 | 15.1 | 57.1 | 5.6 | 11.8 | 60,444 | 62,167 |
| 5 | 35.6 | 20.1 | 20.1 | 75.8 | 7.3 | 15.5 | 79,627 | 78,107 |
| 6 | 8.0 | 3.1 | 3.1 | 14.2 | 2.3 | 4.9 | 18,819 | 17,447 |
| 7 | 14.6 | 6.1 | 6.1 | 26.8 | 4.0 | 8.5 | 29,686 | 30,854 |
| 8 | 23.4 | 10.1 | 10.1 | 43.6 | 6.3 | 13.3 | 44,573 | 46,493 |
| 9 | 34.3 | 15.1 | 15.1 | 64.5 | 9.1 | 19.2 | 64,070 | 63,313 |
| 10 | 45.2 | 20.1 | 20.1 | 85.4 | 11.8 | 25.1 | 82,199 | 77,906 |
| 11 | 11.0 | 3.1 | 3.1 | 17.2 | 3.7 | 7.9 | 20,362 | 20,046 |
| 12 | 20.6 | 6.1 | 6.1 | 32.8 | 6.8 | 14.5 | 33,424 | 34,431 |
| 13 | 33.4 | 10.1 | 10.1 | 53.6 | 11.0 | 23.3 | 51,056 | 50,063 |
| 14 | 49.2 | 15.1 | 15.1 | 79.4 | 16.1 | 34.1 | 70,803 | 65,820 |
| 15 | 65.4 | 20.1 | 20.1 | 105.6 | 21.4 | 45.3 | 82,247 | 78,881 |
| 16 | 13.8 | 3.1 | 3.1 | 20.0 | 5.0 | 10.7 | 21,502 | 22,014 |
| 17 | 26.5 | 6.1 | 6.1 | 38.7 | 9.6 | 20.4 | 35,339 | 37,516 |
| 18 | 43.2 | 10.1 | 10.1 | 63.4 | 15.6 | 33.1 | 52,868 | 53,149 |
| 19 | 64.4 | 15.1 | 15.1 | 94.6 | 23.2 | 49.3 | 70,653 | 68,409 |
| 20 | 86.3 | 20.1 | 20.1 | 126.5 | 31.2 | 66.2 | 81,354 | 80,722 |
| 21 | 20.0 | 3.1 | 3.1 | 26.2 | 8.0 | 16.9 | 23,682 | 26,637 |
| 22 | 38.5 | 6.1 | 6.1 | 50.7 | 15.3 | 32.4 | 38,904 | 42,857 |
| 23 | 61.4 | 10.1 | 10.1 | 81.6 | 24.2 | 51.3 | 56,362 | 58,123 |
| 24 | 95.2 | 15.1 | 15.1 | 125.4 | 37.8 | 80.1 | 72,151 | 73,396 |
| 25 | 131.2 | 20.1 | 20.1 | 171.4 | 52.4 | 111.1 | 84,580 | 85,407 |
| 26 | 25.4 | 3.1 | 3.1 | 31.6 | 10.5 | 22.3 | 23,996 | 29,956 |
| 27 | 50.6 | 6.1 | 6.1 | 62.8 | 21.0 | 44.5 | 39,608 | 47,364 |
| 28 | 87.9 | 10.1 | 10.1 | 108.1 | 36.7 | 77.8 | 58,459 | 64,183 |
| 29 | 133.0 | 15.1 | 15.1 | 163.2 | 55.6 | 117.9 | 75,525 | 78,919 |
| 30 | 175.2 | 20.1 | 20.1 | 215.4 | 73.1 | 155.1 | 91,115 | 90,026 |

Table A3. Resilient modulus data for base layer replicate 3.

| Test Sequence | $\sigma_1$ | $\sigma_2$ | $\sigma_3$ | $\theta$ | $\tau$ | $\sigma_1 - \sigma_3$ | $M_R$ | Pred. $M_R$ |
|---|---|---|---|---|---|---|---|---|
| | psi | psi | psi | psi | psi | psi | Psi | Psi |
| 1 | 6.5 | 3.1 | 3.1 | 12.7 | 1.6 | 3.4 | 19,279 | 16,718 |
| 2 | 11.6 | 6.1 | 6.1 | 23.8 | 2.6 | 5.5 | 29,746 | 29,722 |
| 3 | 18.4 | 10.1 | 10.1 | 38.6 | 3.9 | 8.3 | 43,114 | 45,433 |
| 4 | 26.8 | 15.1 | 15.1 | 57.0 | 5.5 | 11.7 | 61,036 | 62,670 |
| 5 | 35.3 | 20.1 | 20.1 | 75.5 | 7.2 | 15.2 | 80,309 | 78,721 |
| 6 | 8.0 | 3.1 | 3.1 | 14.2 | 2.3 | 4.9 | 19,302 | 18,130 |
| 7 | 14.6 | 6.1 | 6.1 | 26.8 | 4.0 | 8.5 | 30,419 | 31,689 |
| 8 | 23.4 | 10.1 | 10.1 | 43.6 | 6.3 | 13.3 | 45,244 | 47,298 |
| 9 | 34.4 | 15.1 | 15.1 | 64.6 | 9.1 | 19.3 | 65,058 | 63,900 |
| 10 | 45.3 | 20.1 | 20.1 | 85.5 | 11.9 | 25.2 | 83,074 | 78,129 |
| 11 | 10.8 | 3.1 | 3.1 | 17.0 | 3.6 | 7.7 | 21,094 | 20,306 |
| 12 | 20.6 | 6.1 | 6.1 | 32.8 | 6.8 | 14.5 | 34,247 | 35,177 |
| 13 | 33.3 | 10.1 | 10.1 | 53.5 | 10.9 | 23.2 | 51,528 | 50,584 |
| 14 | 49.2 | 15.1 | 15.1 | 79.4 | 16.1 | 34.1 | 70,778 | 65,953 |
| 15 | 65.8 | 20.1 | 20.1 | 106.0 | 21.5 | 45.7 | 81,575 | 78,518 |
| 16 | 14.0 | 3.1 | 3.1 | 20.2 | 5.1 | 10.9 | 22,251 | 23,116 |
| 17 | 26.5 | 6.1 | 6.1 | 38.7 | 9.6 | 20.4 | 35,987 | 38,161 |
| 18 | 43.2 | 10.1 | 10.1 | 63.4 | 15.6 | 33.1 | 53,155 | 53,464 |
| 19 | 64.2 | 15.1 | 15.1 | 94.4 | 23.1 | 49.1 | 70,192 | 68,123 |
| 20 | 86.6 | 20.1 | 20.1 | 126.8 | 31.3 | 66.5 | 80,778 | 79,847 |
| 21 | 20.0 | 3.1 | 3.1 | 26.2 | 8.0 | 16.9 | 24,177 | 27,296 |
| 22 | 38.6 | 6.1 | 6.1 | 50.8 | 15.3 | 32.5 | 39,297 | 43,314 |
| 23 | 61.5 | 10.1 | 10.1 | 81.7 | 24.2 | 51.4 | 56,463 | 58,048 |
| 24 | 95.1 | 15.1 | 15.1 | 125.3 | 37.7 | 80.0 | 72,584 | 72,442 |
| 25 | 132.0 | 20.1 | 20.1 | 172.2 | 52.8 | 111.9 | 84,998 | 83,668 |
| 26 | 25.3 | 3.1 | 3.1 | 31.5 | 10.5 | 22.2 | 24,276 | 30,501 |
| 27 | 50.8 | 6.1 | 6.1 | 63.0 | 21.1 | 44.7 | 40,064 | 47,609 |
| 28 | 88.7 | 10.1 | 10.1 | 108.9 | 37.1 | 78.6 | 58,966 | 63,532 |
| 29 | 132.6 | 15.1 | 15.1 | 162.8 | 55.4 | 117.5 | 76,302 | 77,210 |
| 30 | --- | --- | --- | --- | --- | --- | --- | --- |

Table A4. Resilient modulus data for subbase layer replicate 1.

| Test Sequence | $\sigma_1$ | $\sigma_2$ | $\sigma_3$ | $\theta$ | $\tau$ | $\sigma_1 - \sigma_3$ | $M_R$ | Pred. $M_R$ |
|---|---|---|---|---|---|---|---|---|
| | psi | psi | psi | psi | psi | psi | psi | Psi |
| 1 | 6.5 | 3.1 | 3.1 | 12.7 | 1.6 | 3.4 | 24,736 | 20,095 |
| 2 | 11.6 | 6.1 | 6.1 | 23.8 | 2.6 | 5.5 | 32,010 | 30,918 |
| 3 | 18.4 | 10.1 | 10.1 | 38.6 | 3.9 | 8.3 | 40,732 | 42,315 |
| 4 | 26.9 | 15.1 | 15.1 | 57.1 | 5.6 | 11.8 | 52,627 | 53,684 |
| 5 | 35.6 | 20.1 | 20.1 | 75.8 | 7.3 | 15.5 | 65,857 | 62,919 |
| 6 | 8.0 | 3.1 | 3.1 | 14.2 | 2.3 | 4.9 | 24,090 | 21,258 |
| 7 | 14.6 | 6.1 | 6.1 | 26.8 | 4.0 | 8.5 | 31,066 | 32,133 |
| 8 | 23.4 | 10.1 | 10.1 | 43.6 | 6.3 | 13.3 | 40,493 | 42,956 |
| 9 | 34.3 | 15.1 | 15.1 | 64.5 | 9.1 | 19.2 | 53,305 | 53,144 |
| 10 | 45.2 | 20.1 | 20.1 | 85.4 | 11.8 | 25.1 | 66,238 | 61,062 |
| 11 | 11.0 | 3.1 | 3.1 | 17.2 | 3.7 | 7.9 | 23,540 | 23,310 |
| 12 | 20.6 | 6.1 | 6.1 | 32.8 | 6.8 | 14.5 | 31,022 | 34,159 |
| 13 | 33.2 | 10.1 | 10.1 | 53.4 | 10.9 | 23.1 | 41,788 | 43,852 |
| 14 | 49.1 | 15.1 | 15.1 | 79.3 | 16.0 | 34.0 | 54,934 | 52,482 |
| 15 | 65.7 | 20.1 | 20.1 | 105.9 | 21.5 | 45.6 | 64,574 | 58,845 |
| 16 | 14.0 | 3.1 | 3.1 | 20.2 | 5.1 | 10.9 | 23,284 | 25,072 |
| 17 | 26.5 | 6.1 | 6.1 | 38.7 | 9.6 | 20.4 | 31,978 | 35,771 |
| 18 | 43.2 | 10.1 | 10.1 | 63.4 | 15.6 | 33.1 | 43,498 | 44,939 |
| 19 | 64.3 | 15.1 | 15.1 | 94.5 | 23.2 | 49.2 | 53,827 | 52,502 |
| 20 | 85.5 | 20.1 | 20.1 | 125.7 | 30.8 | 65.4 | 61,813 | 57,794 |
| 21 | 19.9 | 3.1 | 3.1 | 26.1 | 7.9 | 16.8 | 24,485 | 27,992 |
| 22 | 38.4 | 6.1 | 6.1 | 50.6 | 15.2 | 32.3 | 34,919 | 38,287 |
| 23 | 61.0 | 10.1 | 10.1 | 81.2 | 24.0 | 50.9 | 45,040 | 46,268 |
| 24 | --- | --- | --- | --- | --- | --- | --- | --- |
| 25 | --- | --- | --- | --- | --- | --- | --- | --- |
| 26 | --- | --- | --- | --- | --- | --- | --- | --- |
| 27 | --- | --- | --- | --- | --- | --- | --- | --- |
| 28 | --- | --- | --- | --- | --- | --- | --- | --- |
| 29 | --- | --- | --- | --- | --- | --- | --- | --- |
| 30 | --- | --- | --- | --- | --- | --- | --- | --- |

Table A5. Resilient modulus data for subbase layer replicate 2.

| Test Sequence | $\sigma_1$ | $\sigma_2$ | $\sigma_3$ | $\theta$ | $\tau$ | $\sigma_1 - \sigma_3$ | $M_R$ | Pred. $M_R$ |
|---|---|---|---|---|---|---|---|---|
| | psi | psi | psi | psi | psi | psi | Psi | Psi |
| 1 | 6.5 | 3.1 | 3.1 | 12.7 | 1.6 | 3.4 | 22,278 | 18,625 |
| 2 | 11.6 | 6.1 | 6.1 | 23.8 | 2.6 | 5.5 | 30,143 | 28,877 |
| 3 | 18.3 | 10.1 | 10.1 | 38.5 | 3.9 | 8.2 | 38,681 | 39,575 |
| 4 | 26.9 | 15.1 | 15.1 | 57.1 | 5.6 | 11.8 | 50,182 | 50,861 |
| 5 | 35.5 | 20.1 | 20.1 | 75.7 | 7.3 | 15.4 | 61,956 | 59,993 |
| 6 | 8.0 | 3.1 | 3.1 | 14.2 | 2.3 | 4.9 | 22,027 | 19,760 |
| 7 | 14.6 | 6.1 | 6.1 | 26.8 | 4.0 | 8.5 | 29,426 | 30,151 |
| 8 | 23.4 | 10.1 | 10.1 | 43.6 | 6.3 | 13.3 | 38,805 | 40,678 |
| 9 | 34.3 | 15.1 | 15.1 | 64.5 | 9.1 | 19.2 | 50,711 | 50,778 |
| 10 | 45.3 | 20.1 | 20.1 | 85.5 | 11.9 | 25.2 | 62,735 | 58,769 |
| 11 | 10.9 | 3.1 | 3.1 | 17.1 | 3.7 | 7.8 | 21,774 | 21,719 |
| 12 | 20.5 | 6.1 | 6.1 | 32.7 | 6.8 | 14.4 | 29,483 | 32,284 |
| 13 | 33.3 | 10.1 | 10.1 | 53.5 | 10.9 | 23.2 | 40,037 | 42,167 |
| 14 | 49.2 | 15.1 | 15.1 | 79.4 | 16.1 | 34.1 | 52,698 | 50,990 |
| 15 | 65.4 | 20.1 | 20.1 | 105.6 | 21.4 | 45.3 | 62,625 | 57,588 |
| 16 | 14.0 | 3.1 | 3.1 | 20.2 | 5.1 | 10.9 | 21,862 | 23,539 |
| 17 | 26.5 | 6.1 | 6.1 | 38.7 | 9.6 | 20.4 | 30,735 | 34,081 |
| 18 | 43.2 | 10.1 | 10.1 | 63.4 | 15.6 | 33.1 | 42,134 | 43,430 |
| 19 | 64.2 | 15.1 | 15.1 | 94.4 | 23.1 | 49.1 | 52,810 | 51,435 |
| 20 | 85.1 | 20.1 | 20.1 | 125.3 | 30.6 | 65.0 | 61,086 | 57,245 |
| 21 | 19.8 | 3.1 | 3.1 | 26.0 | 7.9 | 16.7 | 23,643 | 26,202 |
| 22 | 38.4 | 6.1 | 6.1 | 50.6 | 15.2 | 32.3 | 34,187 | 36,915 |
| 23 | 61.1 | 10.1 | 10.1 | 81.3 | 24.0 | 51.0 | 44,950 | 45,331 |
| 24 | --- | --- | --- | --- | --- | --- | --- | --- |
| 25 | --- | --- | --- | --- | --- | --- | --- | --- |
| 26 | --- | --- | --- | --- | --- | --- | --- | --- |
| 27 | --- | --- | --- | --- | --- | --- | --- | --- |
| 28 | --- | --- | --- | --- | --- | --- | --- | --- |
| 29 | --- | --- | --- | --- | --- | --- | --- | --- |
| 30 | --- | --- | --- | --- | --- | --- | --- | --- |

Table A6. Resilient modulus data for subbase layer replicate 3.

| Test Sequence | $\sigma_1$ | $\sigma_2$ | $\sigma_3$ | $\theta$ | $\tau$ | $\sigma_1 - \sigma_3$ | $M_R$ | Pred. $M_R$ |
|---|---|---|---|---|---|---|---|---|
| | psi | psi | psi | psi | psi | psi | psi | Psi |
| 1 | 6.5 | 3.1 | 3.1 | 12.7 | 1.6 | 3.4 | 23,166 | 19,352 |
| 2 | 11.6 | 6.1 | 6.1 | 23.8 | 2.6 | 5.5 | 30,536 | 29,734 |
| 3 | 18.4 | 10.1 | 10.1 | 38.6 | 3.9 | 8.3 | 39,415 | 40,698 |
| 4 | 26.9 | 15.1 | 15.1 | 57.1 | 5.6 | 11.8 | 50,911 | 51,688 |
| 5 | 35.5 | 20.1 | 20.1 | 75.7 | 7.3 | 15.4 | 63,222 | 60,697 |
| 6 | 8.0 | 3.1 | 3.1 | 14.2 | 2.3 | 4.9 | 23,349 | 20,493 |
| 7 | 14.5 | 6.1 | 6.1 | 26.7 | 4.0 | 8.4 | 30,120 | 30,939 |
| 8 | 23.3 | 10.1 | 10.1 | 43.5 | 6.2 | 13.2 | 39,292 | 41,467 |
| 9 | 34.3 | 15.1 | 15.1 | 64.5 | 9.1 | 19.2 | 51,626 | 51,457 |
| 10 | 45.3 | 20.1 | 20.1 | 85.5 | 11.9 | 25.2 | 64,292 | 59,276 |
| 11 | 11.0 | 3.1 | 3.1 | 17.2 | 3.7 | 7.9 | 22,802 | 22,517 |
| 12 | 20.5 | 6.1 | 6.1 | 32.7 | 6.8 | 14.4 | 30,076 | 33,046 |
| 13 | 33.3 | 10.1 | 10.1 | 53.5 | 10.9 | 23.2 | 40,567 | 42,816 |
| 14 | 49.2 | 15.1 | 15.1 | 79.4 | 16.1 | 34.1 | 53,371 | 51,427 |
| 15 | 65.4 | 20.1 | 20.1 | 105.6 | 21.4 | 45.3 | 63,109 | 57,788 |
| 16 | 14.0 | 3.1 | 3.1 | 20.2 | 5.1 | 10.9 | 22,647 | 24,268 |
| 17 | 26.5 | 6.1 | 6.1 | 38.7 | 9.6 | 20.4 | 31,019 | 34,773 |
| 18 | 43.3 | 10.1 | 10.1 | 63.5 | 15.7 | 33.2 | 42,479 | 43,953 |
| 19 | 64.2 | 15.1 | 15.1 | 94.4 | 23.1 | 49.1 | 52,894 | 51,674 |
| 20 | 85.2 | 20.1 | 20.1 | 125.4 | 30.7 | 65.1 | 61,108 | 57,212 |
| 21 | 19.9 | 3.1 | 3.1 | 26.1 | 7.9 | 16.8 | 24,192 | 27,128 |
| 22 | 38.4 | 6.1 | 6.1 | 50.6 | 15.2 | 32.3 | 34,546 | 37,470 |
| 23 | 61.0 | 10.1 | 10.1 | 81.2 | 24.0 | 50.9 | 45,318 | 45,619 |
| 24 | --- | --- | --- | --- | --- | --- | --- | --- |
| 25 | --- | --- | --- | --- | --- | --- | --- | --- |
| 26 | --- | --- | --- | --- | --- | --- | --- | --- |
| 27 | --- | --- | --- | --- | --- | --- | --- | --- |
| 28 | --- | --- | --- | --- | --- | --- | --- | --- |
| 29 | --- | --- | --- | --- | --- | --- | --- | --- |
| 30 | --- | --- | --- | --- | --- | --- | --- | --- |

Table A7. Resilient modulus data for subgrade layer replicate 1.

| Test Sequence | $\sigma_1$ | $\sigma_2$ | $\sigma_3$ | θ | τ | $\sigma_1$ - $\sigma_3$ | $M_R$ | Pred. $M_R$ |
|---|---|---|---|---|---|---|---|---|
| | psi | psi | psi | psi | psi | psi | psi | psi |
| 1 | 16.6 | 8.0 | 8.0 | 32.6 | 4.1 | 8.6 | 35,619 | 36,387 |
| 2 | 14.1 | 6.0 | 6.0 | 26.1 | 3.8 | 8.1 | 33,566 | 33,539 |
| 3 | 11.8 | 4.1 | 4.1 | 20.0 | 3.6 | 7.7 | 30,566 | 30,374 |
| 4 | 9.5 | 2.1 | 2.1 | 13.7 | 3.5 | 7.4 | 26,465 | 26,325 |
| 5 | 19.6 | 8.0 | 8.0 | 35.6 | 5.5 | 11.6 | 36,407 | 36,777 |
| 6 | 17.2 | 6.0 | 6.0 | 29.2 | 5.3 | 11.2 | 34,636 | 34,296 |
| 7 | 14.9 | 4.1 | 4.1 | 23.1 | 5.1 | 10.8 | 31,740 | 31,329 |
| 8 | 12.4 | 2.1 | 2.1 | 16.6 | 4.9 | 10.3 | 27,465 | 27,695 |
| 9 | 22.6 | 8.0 | 8.0 | 38.6 | 6.9 | 14.6 | 37,109 | 37,228 |
| 10 | 20.2 | 6.0 | 6.0 | 32.2 | 6.7 | 14.2 | 35,317 | 34,832 |
| 11 | 17.9 | 4.1 | 4.1 | 26.1 | 6.5 | 13.8 | 32,587 | 32,120 |
| 12 | 15.4 | 2.1 | 2.1 | 19.6 | 6.3 | 13.3 | 28,562 | 28,872 |
| 13 | 26.6 | 8.0 | 8.0 | 42.6 | 8.8 | 18.6 | 37,399 | 37,638 |
| 14 | 24.2 | 6.0 | 6.0 | 36.2 | 8.6 | 18.2 | 35,908 | 35,456 |
| 15 | 21.7 | 4.1 | 4.1 | 29.9 | 8.3 | 17.6 | 33,278 | 32,980 |
| 16 | 19.4 | 2.1 | 2.1 | 23.6 | 8.2 | 17.3 | 29,425 | 30,170 |

Table A8. Resilient modulus data for subgrade layer replicate 2.

| Test Sequence | $\sigma_1$ | $\sigma_2$ | $\sigma_3$ | θ | τ | $\sigma_1$ - $\sigma_3$ | $M_R$ | Pred. $M_R$ |
|---|---|---|---|---|---|---|---|---|
| | psi | psi | psi | psi | psi | psi | psi | psi |
| 1 | 16.6 | 8.0 | 8.0 | 32.6 | 4.1 | 8.6 | 39,601 | 39,891 |
| 2 | 14.2 | 6.0 | 6.0 | 26.2 | 3.9 | 8.2 | 35,227 | 35,479 |
| 3 | 11.7 | 4.1 | 4.1 | 19.9 | 3.6 | 7.6 | 30,015 | 30,452 |
| 4 | 9.4 | 2.1 | 2.1 | 13.6 | 3.4 | 7.3 | 25,013 | 24,692 |
| 5 | 19.6 | 8.0 | 8.0 | 35.6 | 5.5 | 11.6 | 40,577 | 40,648 |
| 6 | 17.3 | 6.0 | 6.0 | 29.3 | 5.3 | 11.3 | 37,055 | 36,584 |
| 7 | 14.8 | 4.1 | 4.1 | 23.0 | 5.0 | 10.7 | 32,286 | 31,986 |
| 8 | 12.4 | 2.1 | 2.1 | 16.6 | 4.9 | 10.3 | 26,596 | 26,759 |
| 9 | 22.6 | 8.0 | 8.0 | 38.6 | 6.9 | 14.6 | 41,255 | 41,340 |
| 10 | 20.2 | 6.0 | 6.0 | 32.2 | 6.7 | 14.2 | 38,134 | 37,512 |
| 11 | 17.8 | 4.1 | 4.1 | 26.0 | 6.5 | 13.7 | 33,664 | 33,290 |
| 12 | 15.4 | 2.1 | 2.1 | 19.6 | 6.3 | 13.3 | 28,299 | 28,529 |
| 13 | 26.6 | 8.0 | 8.0 | 42.6 | 8.8 | 18.6 | 41,642 | 42,182 |
| 14 | 24.3 | 6.0 | 6.0 | 36.3 | 8.6 | 18.3 | 39,018 | 38,684 |
| 15 | 21.8 | 4.1 | 4.1 | 30.0 | 8.3 | 17.7 | 34,953 | 34,812 |
| 16 | 19.4 | 2.1 | 2.1 | 23.6 | 8.2 | 17.3 | 30,072 | 30,543 |

Table A9. Resilient modulus data for subgrade layer replicate 3.

| Test Sequence | $\sigma_1$ | $\sigma_2$ | $\sigma_3$ | $\theta$ | $\tau$ | $\sigma_1 - \sigma_3$ | $M_R$ | Pred. $M_R$ |
|---|---|---|---|---|---|---|---|---|
| | psi | psi | psi | psi | psi | psi | psi | Psi |
| 1 | 16.7 | 8.0 | 8.0 | 32.7 | 4.1 | 8.7 | 41,539 | 42,738 |
| 2 | 14.2 | 6.0 | 6.0 | 26.2 | 3.9 | 8.2 | 39,168 | 39,052 |
| 3 | 11.8 | 4.1 | 4.1 | 20.0 | 3.6 | 7.7 | 35,447 | 34,778 |
| 4 | 9.4 | 2.1 | 2.1 | 13.6 | 3.4 | 7.3 | 29,525 | 29,563 |
| 5 | 19.7 | 8.0 | 8.0 | 35.7 | 5.5 | 11.7 | 42,453 | 43,196 |
| 6 | 17.2 | 6.0 | 6.0 | 29.2 | 5.3 | 11.2 | 40,329 | 39,804 |
| 7 | 14.9 | 4.1 | 4.1 | 23.1 | 5.1 | 10.8 | 36,704 | 35,968 |
| 8 | 12.5 | 2.1 | 2.1 | 16.7 | 4.9 | 10.4 | 31,047 | 31,384 |
| 9 | 22.5 | 8.0 | 8.0 | 38.5 | 6.8 | 14.5 | 43,348 | 43,580 |
| 10 | 20.2 | 6.0 | 6.0 | 32.2 | 6.7 | 14.2 | 41,070 | 40,465 |
| 11 | 17.8 | 4.1 | 4.1 | 26.0 | 6.5 | 13.7 | 37,528 | 36,923 |
| 12 | 15.4 | 2.1 | 2.1 | 19.6 | 6.3 | 13.3 | 32,221 | 32,797 |
| 13 | 26.6 | 8.0 | 8.0 | 42.6 | 8.8 | 18.6 | 43,849 | 44,082 |
| 14 | 24.2 | 6.0 | 6.0 | 36.2 | 8.6 | 18.2 | 41,879 | 41,232 |
| 15 | 21.8 | 4.1 | 4.1 | 30.0 | 8.3 | 17.7 | 38,387 | 38,048 |
| 16 | 19.4 | 2.1 | 2.1 | 23.6 | 8.2 | 17.3 | 33,573 | 34,413 |

# REPORT DOCUMENTATION PAGE

*Form Approved OMB No. 0704-0188*



| **1. REPORT DATE** *(DD-MM-YYYY)* | **2. REPORT TYPE** | **3. DATES COVERED** *(From - To)* |
|---|---|---|
| August 2013 | Final report | |

**4. TITLE AND SUBTITLE**

Comparing Production and Placement of Warm-Mix Asphalt to Traditional Hot-Mix Asphalt for Constructing Airfield Pavements

**5a. CONTRACT NUMBER**

**5b. GRANT NUMBER**

**5c. PROGRAM ELEMENT NUMBER**

**6. AUTHOR(S)**

John F. Rushing, Mariely Mejías-Santiago, and Jesse D. Doyle

**5d. PROJECT NUMBER**

**5e. TASK NUMBER**

**5f. WORK UNIT NUMBER**

**7. PERFORMING ORGANIZATION NAME(S) AND ADDRESS(ES)**

Geotechnical and Structures Laboratory
US Army Engineer Research and Development Center
3909 Halls Ferry Road
Vicksburg, MS 39180-6199

**8. PERFORMING ORGANIZATION REPORT NUMBER**

ERDC/GSL TR-13-35

**9. SPONSORING / MONITORING AGENCY NAME(S) AND ADDRESS(ES)**

US Air Force Civil Engineer Center
139 Barnes Drive, Suite 1
Tyndall AFB, FL 32403-5319

**10. SPONSOR/MONITOR'S ACRONYM(S)**

**11. SPONSOR/MONITOR'S REPORT NUMBER(S)**

**12. DISTRIBUTION / AVAILABILITY STATEMENT**

Approved for public release; distribution is unlimited.

**13. SUPPLEMENTARY NOTES**

**14. ABSTRACT**

Warm-mix asphalt (WMA) is an emerging technology that allows for production and placement of asphalt concrete at lower temperatures than conventional hot-mix asphalt (HMA). Full-scale pavement test sections were constructed using conventional equipment to observe differences in the techniques used to produce, place, and compact asphalt concrete using warm mixtures. These observations are needed to ensure construction specifications are adjusted appropriately for WMA construction. Results from this phase of the study include data identifying differences in WMA and HMA construction. The WMA was successfully constructed using the same equipment to produce in-place density equivalent to the HMA at reduced temperatures. Future work will include trafficking the pavement sections using accelerated pavement testing equipment to determine the WMA rutting performance.

**15. SUBJECT TERMS**

| | | |
|---|---|---|
| Warm Mix Asphalt | Asphalt | Pavement construction |
| | Accelerated pavement testing | |

| **16. SECURITY CLASSIFICATION OF:** | | | **17. LIMITATION OF ABSTRACT** | **18. NUMBER OF PAGES** | **19a. NAME OF RESPONSIBLE PERSON** |
|---|---|---|---|---|---|
| **a. REPORT** | **b. ABSTRACT** | **c. THIS PAGE** | | 79 | **19b. TELEPHONE NUMBER** *(include area code)* |